THESIS APPROVAL

GRADUATE SCHOOL, KASETSART UNIVERSITY

Master of Science (Chemistry)
DEGREE

Physical Chemistry   Chemistry
FIELD   **DEPARTMENT**

TITLE: The Protein Framework and Solvent Effect on the Energetics of the Acylation Step in Butyrylcholinesterase-catalyzed Hydrolysis of Cocaine: An Electronic Embedding Method

NAME: Mr. Narongsak Arayalert

THIS THESIS HAS BEEN ACCEPTED BY

_____ **THESIS ADVISOR**
(Professor Jumras Limtrakul, Ph.D.   )

_____ **COMMITTEE MEMBER**
(Mr. Tanin Nanok, Ph.D.   )

_____ **COMMITTEE MEMBER**
(Assistant Professor Prachumporn Kongsaeree, Ph. D.   )

_____ **DEPARTMENT HEAD**
(Assistant Professor Noojaree Prasitpan, Ph.D.   )

APPROVED BY THE GRADUATE SCHOOL ON _____

_____ **DEAN**
(Associate Professor Vinai Artkongharn, M.A.   )

THESIS

THE PROTEIN FRAMEWORK AND SOLVENT EFFECT ON THE ENERGETICS OF THE ACYLATION STEP IN BUTYRYLCHOLINESTERASE-CATALYZED HYDROLYSIS OF COCAINE: AN ELECTRONIC EMBEDDING METHOD

NARONGSAK ARAYALERT

A Thesis Submitted in Partial Fulfillment of
the Requirements for the Degree of
Master of Science (Chemistry)
Graduate School, Kasetsart University
2007

Narongsak Arayalert 2007: The Protein Framework and Solvent Effect on the Energetics of the Acylation step in Butyrylcholinesterase-catalyzed Hydrolysis of Cocaine: An Electronic Embedding Method. Master of Science (Chemistry), Major Field: Physical Chemistry, Department of Chemistry. Thesis Advisor: Professor Jumras Limtrakul, Ph.D. 82 pages.

The geometry parameters of the transition state, intermediate, and prereactive enzyme-substrate complex was optimized at B3LYP/6-31G(d,p) level of theory in the cluster model and the cluster amino model and the corresponding energy barriers have been studied by performing the polarizable continuum model (PCM) and the embedded calculations on the first step of acylation process considered by single point calculation at B3LYP/6-31G(d,p) level of theory 6.71 and 5.07 kcal/mol, respectively and B3LYP/6-31++G(d,p) level of theory 4.51 and 3.75 kcal/mol, respectively. The energy barriers decreased from the cluster amino model by approximately 0.9-2.0 kcal/mol. These calculations allow us to account for the electrostatic interaction of protein environment effects and solvent effects on the pathway and the energy barriers of these enzymatic reactions. This shows the protein environment effect significantly influences the hydrogen bonding between the oxyanion hole and the carbonyl oxygen of cocaine. These computational results provide valuable insights into the future design of BChE mutants with a higher catalytic activity for cocaine.

_____	_____	___	/	___	/ ___
Student's signature	Thesis Advisor's signature				

ACKNOWLEDGEMENTS

Narongsak Arayalert

April 2007

TABLE OF CONTENTS

Page

LIST OF TABLES

LIST OF FIGURES

LIST OF ABBREVIATIONS

Ach	=	Acetylcholine
AChE	=	Acetylcholinesterase
AM1	=	Austin model 1
BCh	=	Butyrylcholine
B3LYP	=	Beck's three parameter hybrid functional using the LYP correlation functional
BChE	=	Butyrylcholinesterase
BTC	=	Butyrylthiocholine
ChE	=	Cholinesterase
CS	=	Catalytic substrate binding site
DFT	=	Density functional theory
ES	=	Enzyme substrate complex
EVB	=	Emppirical valence bond
HF	=	Hartree-Fock
IMOMM	=	Integrated molecular orbital and molecular mechanics method
INT	=	Intermediate
kcal/mol	=	Kilocalorie per mol
LBHBs	=	Low-barrier hydrogen bonds
LYP	=	Lee-Yang-Parr functional
MD	=	Molecular dynamics
MM	=	Molecular mechanics
MM-PB	=	Molecular-mechanics-Poisson-Boltzmann
MO	=	Molecular orbital
MP2	=	The second-order MØller-Plesset perturbations theory
ONIOM	=	Our-own-N-layered Integrated molecular Orbital and molecular Mechanics
PAS	=	The peripheral anionic site
PCM	=	Polarizable continuum method
PM3	=	Paranetric method number 3

QM	=	Quantum mechanics
QM/MM	=	Quantum mechanical/molecular mechanical
OPs	=	Organophosphates
SCRF	=	Self-consistent reaction field
SIMOMM	=	Surface Integrated Molecular Orbital/Molecular Mechanics
*Tc*AChE	=	*Torpedo californica* Acetylcholinesterase
TS	=	Transition state

AMINO ACID CODES

Ala	=	Alanine
Val	=	Valine
Leu	=	Leucine
Ile	=	Isoleucine
Pro	=	Proline
Phe	=	Phenylanaline
Trp	=	Trptophan
Met	=	Methionine
Gly	=	Glycine
Ser	=	Serine
Thr	=	Threonine
Cys	=	Cysteine
Tyr	=	Tyrocine
Asn	=	Asparagine
Gln	=	Glutamine
Asp	=	Aspartic acid
Glu	=	Glutamic acid
Lys	=	Lysine
Arg	=	Arginine
His	=	Histidine

THE PROTEIN FRAMEWORK AND SOLVENT EFFECT ON THE ENERGETICS OF THE ACYLATION STEP IN BUTYRYLCHOLINESTERASE-CATALYZED HYDROLYSIS OF COCAINE: AN ELECTRONIC EMBEDDING METHOD

INTRODUCTION

Cholinesterases are widespread enzymes in the cholinergic and noncholinergic, also in plasma and other body fluids. There are two types of cholinesterases: acetylcholinesterase (AChE) and butyrylcholinesterase (BChE), which can be distinguished by their substrate and inhibitor properties. The role of acetylcholinesterase is to breakdown the neurotransmitter acetylcholine into choline and acetic acid at the synaptic cleft, and then the nerve impulse is transmitted across to the synaptic gap (Massoulie *et al*., 1993). In addition, both AChE and BChE have roles that are independent of their catalytic activities, such as cell differentiation and development (Behra *et al*., 2002; Meshorer *et al*., 2002). The catalytic mechanism of AChE is extremely efficient in approaching diffusion-controled rates (Quinn, 1987). The crystal structure of the *Torpedo californica* acetylcholinesterase (*Tc*AChE) showed that the active site catalytic triad, consisting of Ser200-His440-Glu327, is at the bottom of the aromatic gorge in the protein at a depth of approximately 20 Å (Sussman *et al*., 1991). One of the most interesting parts in this enzyme is the peripheral anionic site (PAS) at the edge of the aromatic gorge (Barak *et al*., 1994 and Szegletes *et al*., 1999). The PAS has the ability to bind many different types of substrate, and effect the conformational change of the active center. The studies suggested that substrate moves slowly to the acyl binding site by the binding of the ligand to the PAS. (Szegletes *et al*., 1999; De Gerrari *et al*., 2001). Although a peripheral anionic site of human BChE, the studies showed that its location and the function depends on the significant difference of the ligand bindings from those of AChE (Masson *et al*., 1997; Nachon *et al*., 1998).

A result from the binding between PAS and substrate, is that it leads the flexible arms of the Ω loop to come closer together and for the substrate to slide down to the choline binding site of the active site gorge. This is the site in which the positively charged quaternary ammonium of ester substrate is found at the middle of the active site gorge, between the peripheral and acyl binding sites. It is not clear what role the residues which are concerned in binding with substrate play in this site. But, there are many studies on the crystal structure and labeling experiments which show that positively charged quaternary ammonium of ester substrate form the cation-π complex with Phe82 (Masson *et al.*, 1997; Masson *et al.*, 1999; Masson *et al.*, 2001).

The physiological role of BChE is still unknown (Chatonnet and Lockridge, 1989; Mack and Robitzki, 2000). Although unreal substrates are not clear, BChE can hydrolyze carboxylic or phosphoric acid ester compounds, including acetylcholine and other acylcholines. Loss of activity of AChE leads to abnormal signs and symptoms, which include the complete loss of muscle activity for one or more muscle groups, called muscle paralysis, seizure and may cause death. BChE is another choice of detox anticholinesterase compounds. It detoxifies anticholinesterase compounds before they reach AChE target sites. Therefore, it has important pharmacological and toxicological roles (Lockridge and Masson, 2000). For example, BChE acts as a preventer against neurotoxic organophosphates such as soman, tabun, and sarin, which can be used as nerve gasses against civilian or military populations (Allon *et al*., 1998; Broomfield *et al*., 1991; Raveh *et al*., 1993).

BChE is one of the most important enzymes needed for suitable activity in the nervous systems of vertebrates, insects, and humans because it will breakdown the neurotransmitter at the synaptic cleft, and then the nerve impulse is transmitted across to the synaptic gap. Chemical classes of pesticides, such as organophosphates, and other chemical classes, such as cocaine, work against undesirable targets by interfering with or inhibiting the enzyme and lead to the production of chemical products which can be toxic

to humans.

Cocaine is still an important public health problem the world over and this is further compounded by the increasing number of addicts. The effects of cocaine in the short-term result in many symptoms such as decreased appetite, increased body temperature, heart rate, blood pressure, constricted blood vessels and dilated pupils. Long-term effects are addiction, followed by many health problems. Overdoses of cocaine lead to the severe impairment of the respiratory and cardiovascular systems and, consequently, death is the result. There have been many investigations that have proposed treatment through roles that interfere with cocaine. A classical approach is to use small molecules to interfere between the cocaine and a receptor, but this method has had limited success as it is difficult to block only antibodies or peptide ligands. (Landry *et al.,* 1997*;* Gorelick, 1997; Spanrenberg *et al.*, 1997; Carroll *et al.,* 1999 and Singh, 2000).

The next approach is developed by using a cocaine antibody that strongly blocks cocaine in the blood stream before it binds with the receptor in the cenral nervous system (Fox, 1997). However, a failing of this strategy is that its capability of binding is only sufficient when a high dosage of cocaine is the target. A more effective method to degrade cocaine is to use an anti-cocaine catalytic antibody, which is sufficiently hydrolyzed cocaine, that strongly binds and degrades the cocaine. An anti-cocaine catalytic antibody that can be used as a therapeutic agent is butyrylcholinesterase, a natural cocaine esterase. Clinical studies suggest that BChE has many advantages. Firstly, human BChE has been in clinical useage for a long time and there are no harmful effects when BChE plasma activity is increased. Secondly, about 20 different mutants of human BChE occur in nature, with no change to the genetics having been identified (Lockridge *et al.,* 1997). For these reasons, the metabolism of cocaine by hydrolyzing BChE is considered a good sign in the pharmacokinetic approach for the treatment of cocaine abuse and dependence (Gorelick, 1997).

For the enzymatic reaction of BChE-catalyse hydrolysis of cocaine, the active site of the enzyme, the catalytic triad, consists of Ser198, His438, and Glu325, which are similar to the catalytic triad in the other serine hydrolases (Warshel and Ressell, 1986; Sholten et al.,1988; Warshel et al., 1989; Daggett et al., 1991; Gerlt and Gassman, 1993; Cleland and Kreevoy, 1994; Frey et al., 1994; Golubev et al., 1994 and Hu et al., 1998). The enzyme has a 25 Å deep and narrow active site gorge in which there are about 55 residues. The OH group of Ser198 has more nucleophilic via the proton acceptor of His438 and is able to attack the carbonyl carbon of the ester substrate by the nucleophilic oxygen of Ser198. The reaction pathway is divided into two steps: acylation and deacylation. The acylation step is initiated by forming a tetrahedral imtermediate (INT1) through the first transition state (TS1), then His438 is deprotonated as the alcoholic part of the ester leaves the group. The next step is the deacylation step, which is a base-catalyzed reaction hydrolysis involving a water molecule. The mechanism involves a double-proton transfer mechanism, a process of transferring between two protons simultaneously in the transition state. One proton transfers along the hydrogen bond between Ser198 and His438 while the other transfers from another proton of His438 to Glu325.

It is of interest to study the energy barrier for BChE-catalyzed hydrolysis of the cocaine pathway in aqueous solution because most of the chemical and biochemical processes occur in this solution. The solvent often affects the rate of reaction in most reactions. The energy barrier of the reaction will be decreased or the transition state will be lowered. The calculation of the reaction pathway for the hydrolysis of cocaine in aqueous solution has been the subject of studies (Zhan et al., 2001; Rylander et al.,1950).

The enzyme usually possesses thousands of atoms per unit cell, sometimes making the use of sophisticated methods computationally too expensive and impractical when very large structures are concerned. The recent development of hybrid methods, notably the embedded method, has brought a larger system within reach of obtaining

accurate results. At the present time, the embedded method is applied to the study of extended systems (Sinclair *et al.,* 1998; Limtrakul *et al.,* 2001; Lomratsiri *et al.,* 2001; Treesukol *et al.,* 2001; Ketrat *et al.*, 2003; Jansang *et al.,* 2006). This is the first time that the embedded method is being used in a biomolecule form in which the effect of the framework can significantly change the energy of the system as part of the long-range interaction. The electronic properties of the enzyme are modeled with quantum chemical methods for relatively small clusters where the reaction occurs in the active site.

We are attempting to determine the energy barrier for the acylation step of BChE-catalyzed hydrolysis of the cocaine mechanism in aqueous solution by carrying out polarizable continuum model (PCM) calculations, and long-range electrostatic interactions are expected to contribute significantly to the reaction pathway. In the following section, we describe the cluster models and methods of calculation and the geometrical differences in the active site region between the different models. All computational results for the acylation pathway will be presented.
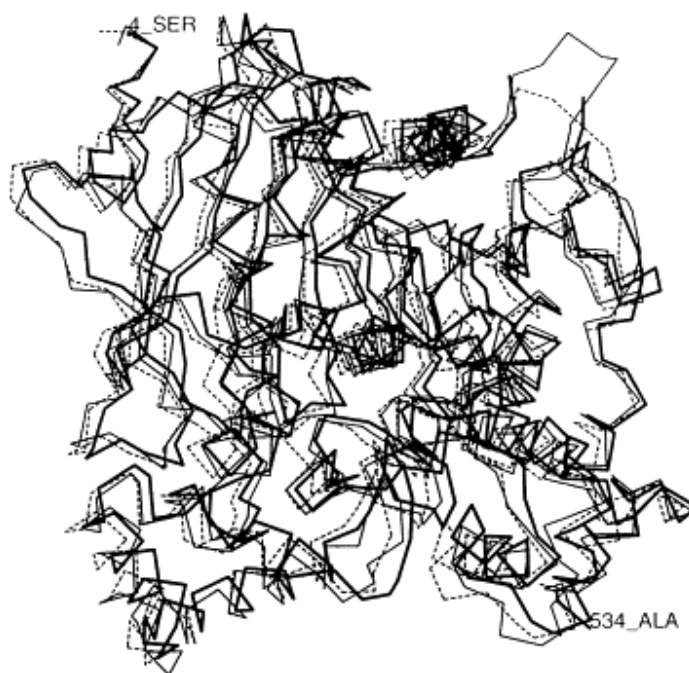
Figure 1   Superimposition of AChE (—), BChE (homology model) (—) and BChE (generated by MODELLER) (--). The three dimensional structures are displayed as C_α traces. The amino acid coding refers to AChE. A computer model of BChE was constructed starting from the coordinates of AChE at 2.8 Å resolution (Sussman *et al.,* 1991). Residues 4-534 of AChE were successfully aligned with residues 2-532 of BChE with no deletions or additions. The missing residues 483-487, Thr-Gln-Asn-Asn-Ser, in the loop were modeled on a fragment obtained from a PDB search. The last amino acids 533-574 were not built into the model, because they were deemed to be insignificant for the investigation of the active site. To compare the result of the comparative modeling the MODELLER program was used to build a model of BChE. Hydrogen atoms were added to the BChE models in standard geometries, before energy minimization.
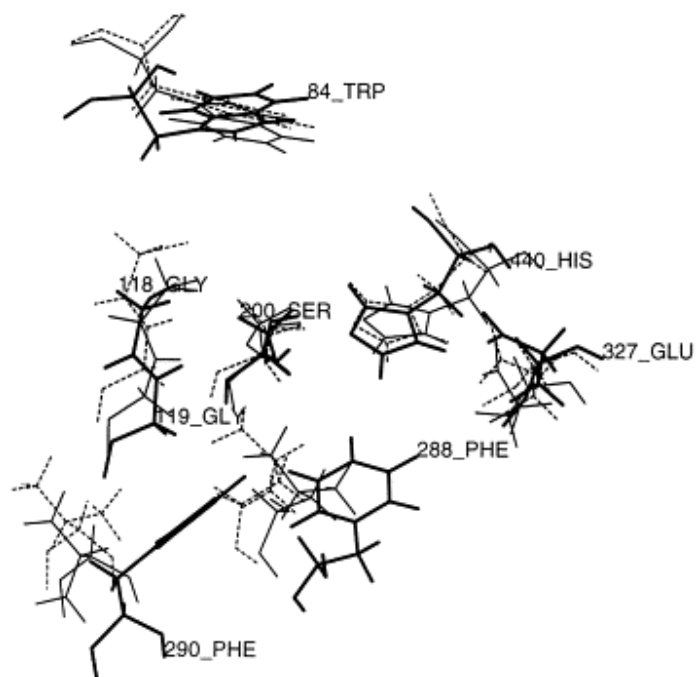
Figure 2 The active site regions of superimposed structures of TcAChE (refined structure) (—), BChE (homology model) (—) and BChE (generated by MODELLER) (--). The amino acid coding refers to TcAChE (Ekholm, 1999).
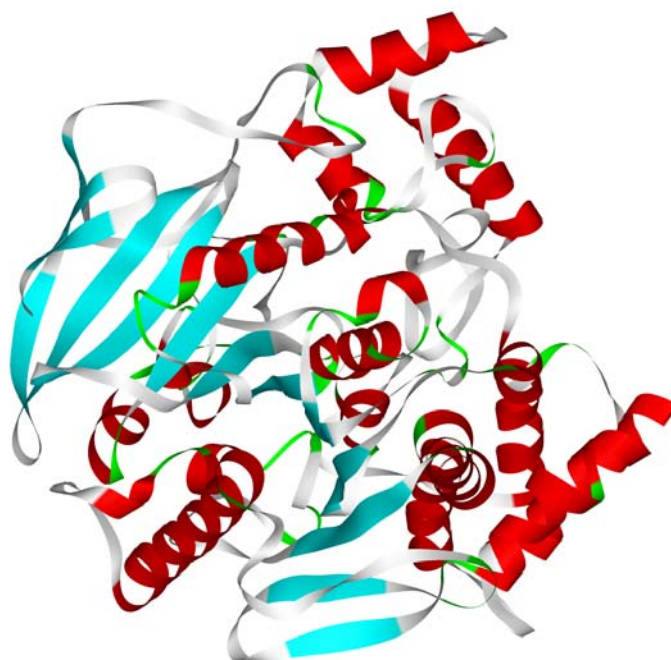
Figure 3 The three-dimensional structure of butyrylcholinesterase
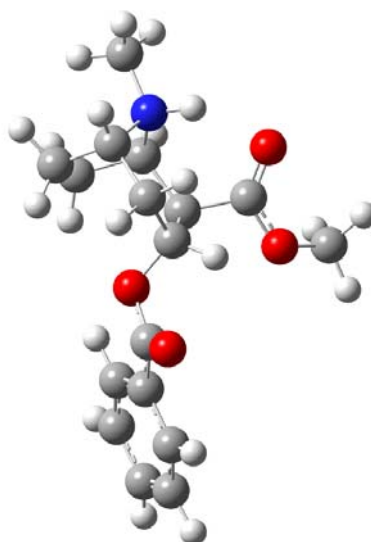
Figure 4 Structure of (-)-cocaine

LITERATURE REVIEW

Cocaine is a drug subject to frequent abuse: with overdose, the effects of which include respiratory depression, cardiac arrthythmia, and acute hypertension (Sparenborg *et al.*, 1997). These effects have led to the development of an effective treatment. The first approach, that sought small molecules to interfere with the cocaine-receptor interaction failed because it was difficult to block the interaction between cocaine and the receptor (Landry and Yang, 1997; Singh, 2000; Sparenborg *et al.*, 1997; Gorelick, 1997). Next, (Fox *et al.*, 1997) devoloped the approach of anti-cocaine catalytic antibodies. These can bind tightly to cocaine, preventing it from crossing the blood barrier in the brain. Stefan and others explored the binding site of the novel human anti-cocaine mAb using a set of 39 cocaine analogues and 3D-QSAR techniques (Stefan *et al.*, 2004) . The antibody has a high cocaine affinity and specificity and is, therefore, a good prototype for a therapeutic agent against cocaine addiction and relapse. For the pharmacological therapy of cocaine addiction, a number of treatment strategies have been pursued (Carroll *et al.*, 1999).

In a more potent therapy, cocaine is blocked by the adminstration of a catalytic antibody, an artificial enzyme that can bind and degrade cocaine (Landry *et al.*, 1997; Landry *et al.*, 1993; Yang *et al.*, 1996). The catalytic antibody that was developed is the cocaine-hydrolyzed enzyme in humans, butyrylcholinesterase (BChE). It is suggested that BChE is a unique enzyme and different from the other enzymes in that, firstly, BChE has a long history of clinical use and no adverse effects have been noted with increased BChE plasma activity. Secondly, about 20 mutants of BChE are obviously not antigenic (Lockridge *et al.*, 1997).

The fundamental reaction mechanisms for cocaine hydrolysis in human butyrylcholinesterase have been investigated by using QM calculations (Zhan *et al.*, 2003). The fundamental catalytic hydrolysis pathway, consisting of acylation and

deacylation stages similar to those for ester hydrolysis by other serine hydrolyses, was proposed on the basis of the simulated prereactive complex and comfirmed theoretically by ab initio reaction coordinate calculations. Both the acylation and deacylation follow a double-proton-transfer mechanism.

Two types of cholinesterase that are acetylcholinesterase (AChE) and butyrylcholinesterase (BChE) are capable of hydrolyzing the neurotransmitter acetylcholine in humans. Although the primary structures of AChE and BChE are alike, being 73% homologous and 54% identical (Aldrige, 1953; Silman and Giamberardino, 1979) found that the molecular forms differ in the number of catalytic subunits, in their level of hydrophobicity (Ott, 1985) and mode of glycosylation (Rotundo, 1984) and in their cellular and subcellular localization (Massoulie and Bon, 1982).

Like BChE, the synaptic enzyme acetylcholinesterase (AChE) which terminates transmission at the cholinergic synapses by rapidly hydrolysing acetylcholine was investigated (Silman *et al.*, 1999). It was found that it anchored within the synaptic cleft by a highly specialized anchoring device in which catalytic subunit tetramers assemble around a polyproline II helix. AChE is the target of nerve agents, insecticides and therapeutic drugs, in particular the first generation of anti-Alzheimer drugs. Both target-guided synthesis and structure-based drug design have been used effectively to obtain potent anticholinesterase agents. In addition, AChE is believed to play 'non-classical' roles in addition to its 'classical' role in terminating synaptic transmission (e.g. as an adhesion protein). It also accelerates the assembly of Abeta into amyloid fibrils. Both of these actions involve the so-called 'peripheral' anionic site at the entrance to the active-site gorge. Novel anticholinesterases are targeted against this site, rather than against the active site at the bottom of the gorge.

The electrostatic potentials for the three-dimensional structures of cholinesterases from various species were calculated, using the Delphi algorithm, on the basis of the Poisson–Boltzmann equation. The structures for *Torpedo californica* and mouse

acetylcholinesterase, were used to build homology models of the human, *Bungarus fasciatus,* and *Drosophila melanogaster* acetylcholinesterases and human butyrylcholinesterase (Felder *et al.*, 1997). All the structures reveal a negative external surface potential, in the area around the entrance to the active-site gorge, that become more negative as the rim of the gorge is approached. Moreover, the potential becomes increasingly more negative along the central axis running down the gorge, and is largest at the base of the gorge, near the active site. Ten key acidic residues conserved in the sequence alignments of AChE from various species, both in the surface area near the entrance of the active-site gorge and at its base, appear to be primarily responsible for these potentials. The potentials are highly correlated among the structures examined, down to sequence identities as low as 35%. This indicates that they are a conserved property of the cholinesterase family, and could serve to attract the positively charged substrate into and down the gorge to the active site, and may play other roles important for the cholinesterase function.

The Brownian dynamics simulations of the encounter kinetics between the active site of the wild-type and Glu-199 mutant of *Torpedo californica* acetylcholinesterase (TcAChE) with a charged substrate were performed (Wlodek and Antosiewwicz, 1997). In addition, ab initio quantum chemical calculations using the 3-21G basis set were undertaken to probe the energetics of the transformation of the Michaelis complex into a covalently bound tetrahedral intermediate using various models of the wild-type and Glu-199Gln mutant active sites. The quantum calculations predicted a factor of 32 reduction in the rate of formation of the tetrahedral intermediate upon the Glu-199Gln mutation and showed that the Glu-199 residue located in the proximity of the enzyme active triad boosts AChE's activity in a dual fashion: (1) by increasing the encounter rate due to the favorable modification of the electric field inside the enzyme reaction gorge and (2) by stabilization of the transition state for the first chemical step of catalysis. Their calculations also demonstrate the critical role of the oxyanion hole in stabilization of the tetrahedral intermediate and suggests that a charge relay mechanism may operate in the

Glu-199Gln mutant AChE as opposed to a general base mechanism as in the wild-type enzyme.

Also, The structure of a complex of *Torpedo californica* acetylcholinesterase with the transition state analog inhibitor *m*-(*N,N,N*-trimethylammonio)-2,2,2-trifluoroacetophenone has been solved by X-ray crystallographic methods to 2.8 Å resolution (Harel *et al.*, 1997). Since the inhibitor binds to the enzyme about 10^{10}-fold more tightly than the substrate acetylcholine, this complex provides a visual accounting of the enzyme-ligand interactions that provide the molecular basis for the catalytic power of acetylcholinesterase. The carbonyl carbon of the trifluoroketone function interacts covalently with Ser-200 of the Ser-200-His-440-Glu-327 catalytic triad. The acetyl ester hydrolytic specificity of the enzyme is revealed by the interaction of the CF_3 function of the transition state analog with a concave binding site comprised of the residues Cys-119, Trp-233, Phe-288, Phe-290, and Phe-331. The highly geometrically convergent array of enzyme-ligand interactions visualized in the complex described herein envelopes the acylation transition state and sequesters it from the solvent, this being consistent with the location of the active site at the bottom of a deep and narrow gorge.

Most of the theoretical work on the catalytic mechanism of cholinesterases has been carried out on the AChE enzyme to understand the origin of its remarkable rate enhancement. The accurate modeling of biological processes presents major computational difficulties owing to the inherent complexity of the macromolecular systems of interest. Simulations of biochemical reactivity tend to require highly computationally intensive quantum mechanical methods, but localized chemical effects tend to depend significantly on the properties of the extended biological environment - a regime far more readily examined with lower-level classical empirical models. Mixed quantum/classical techniques are gaining in popularity as a means of bridging these competing requirements. The presented results, compared two quantum mechanics/molecular mechanics implementations (the SIMOMM technique of Gordon et al. as implemented in GAMESS, and the ONIOM technique of Morokuma *et al.*, found in

Gaussian 98) as performed on the enzyme acetylcholinesterase and model nerve agents (Hurley *et al.*, 1997). Their work represents part of the initial phase of a DoD HPCMP Challenge project in which they attempted to reliably characterize the biochemical processes responsible for nerve agent activity and inhibition, thereby allowing predictions on compounds unrelated to those already studied. Additionally, the study of the dynamics of ligand movement through the constricted region of the acetylcholinesterase gorge that is important to understand how the ligand gains access to and is released from the active site of the enzyme. Molecular dynamics simulations of the simple ligand, tetramethylammonium, crossing this bottleneck region are conducted using umbrella potential sampling and activated flux techniques. The low potential of mean force obtained is consistent with the fast reaction rate of acetylcholinesterase observed experimentally. From the results of the activated dynamics simulations, local conformational fluctuations of the gorge residues and larger scale collective motions of the protein are found to correlate highly with the ligand crossing (Bui *et al.*, 2003).

The 10-ns MD simulation of mAChE was equilibrated and stable as shown by various properties and energy components and gave reasonable *B* factors. The small fraction of the total number of frames in which an open back door is observed severely limits the statistics of our analysis. Back-door opening seems to prefer certain dihedral angle values for some of the residues in the region (Tai *et al.*, 2001). They developed the porcupine plots to visualize the concerted motions between residues in AChE and the gorge width. The plots show that residues lining the gorge have the largest velocity covariance with the gorge, and residues in the same moiety as the gorge move concertedly away from the gorge when it opens. This clearly reveals the residues involved in gorge opening and gives the magnitude and direction of such involvement. They found that the Phe-338 Ce2-Tyr124 OH distance is highly predictive of the gorge proper radius; the corresponding a-carbon distance has a moderate correlation. Principal component analysis showed that the gorge proper radius is determined by motions on many different length scales; this is likely to be related to the fractal dynamics model they previously proposed.

The catalytic mechanism of BChE has been investigated by mutagenesis and kinetic experiments using different substrates. Butyrylcholinesterase is a serine esterase, closely related to acetylcholinesterase. Both enzymes employ a catalytic triad mechanism for catalysis, similar to that used by serine proteases such as α-chymotrypsin. Enzymes of this type are generally considered to be inactive at pH values below 5, because the histidine member of the catalytic triad becomes protonated (Masson *et al.*, 2003). This work found that butyrylcholinesterase retains activity at pH ≤5, under conditions of excess substrate activation. This low-pH activity appears with wild-type butyrylcholinesterase as well as with all the mutants we examined: Ala-328G, Ala-328I, Ala-328F, Ala-328Tyr, Ala-328Trp, Glu-197Gln, Leu-286Trp, Val-288Trp and Tyr-332Ala (residue Ala-328 is at the bottom of the active-site gorge, near the π-cation-binding site; Glu-197 is next to the active-site serine Ser-198; Leu-286 and Val-288 form the acyl-binding pocket; and Tyr-332 is a component of the peripheral anionic site). For example, the k_{cat} value at pH 5.0 for activity in the presence of excess substrate was 32 900 ± 4400 min⁻¹ for wild-type, 55 200 ± 1600 min⁻¹ for Ala-328Phe, and 28 700 ± 700 min⁻¹ for Ala-328Trp. This activity is titratable, with pK_a values of 6.0–6.6, suggesting that the catalytic histidine is protonated at pH 5. The existence of activity when the catalytic histidine is protonated indicates that the catalytic-triad mechanism of butyrylcholinesterase does not operate for catalysis at low pH. The mechanism explaining the catalytic behaviour of butyrylcholinesterase at low pH in the presence of excess substrate remains to be elucidated.

Tetraalkylammonium (TAA) salts are well known reversible inhibitors of cholinesterases. However, at concentrations around 10 mm, they were found to activate the hydrolysis of positively charged substrates, catalyzed by wild-type human butyrylcholinesterase (Stojan *et al.*, 2002). The presented study was undertaken to determine whether the peripheral anionic site (PAS) of human BChE and/or the catalytic substrate binding site (CS) are involved in this phenomenon. For this purpose, the kinetics

of butyrylthiocholine (BTC) hydrolysis by wild-type human BChE, by selected mutants and by horse BChE was carried out at 25 °C and pH 7.0 in the presence of tetraethylammonium (TEA). It appeared that human enzymes with more intact structure of the PAS showed more prominent activation phenomenon. The following explanation has been put forward: TEA competes with the substrate at the peripheral site, thus inhibiting the substrate hydrolysis at the CS. As the inhibition by TEA is less effective than the substrate inhibition itself, it mimics activation. At concentrations around 40 mm, well within the range of TEA competition at both substrate binding sites, it lowers the activity of all tested enzymes.

The effect of hydrostatic and osmotic pressures on the aging process (dealkylation of an isopropyl chain) of phosphorylated enzymes [di-isopropylated (DIP)-BChE] was investigated (Masson *et al.*, 2003). Hydrostatic pressure markedly increased the rate of aging of wild-type enzyme. The average activation volume (DeltaV(not equal)) for the dealkylation reaction was -170 ml/mol for DIP wild-type BChE. On the other hand, hydrostatic pressure had little effect on the aging of the DIP mutants (DeltaV(not equal) = -2.6 ml/mol for Glu-197Asp and -2 ml/mol for Asp-70Gly), suggesting that the transition state of the aging process was associated with an extended hydration and conformational change in wild-type BChE, but not in the mutants. The rate of aging of wild-type and mutant enzymes decreased with osmotic pressure, allowing very large positive osmotic activation volumes (DeltaV not equal to osm) to be estimated, thus probing the participation of water in the aging process. Molecular dynamics simulations performed on the active-site gorge of the wild-type DIP adduct showed that the isopropyl chain involved in aging was highly solvated, supporting the idea that water is important for stabilizing the transition state of the dealkylation reaction. Wild-type BChE was inhibited by soman (pinacolyl methylphosphonofluoridate). In a similar work, (Masson *et al.*, 1996) determined what amino acids at the mouth of the active-site gorge are important for the function of human butyrylcholinesterase. Mutants Asp-70Gly, Glu-119Try, Gly-283Asp, Ala-277Trp, Ala-277His and Ala-277Trp/Gly-283Asp were

expressed in human embryonal kidney cells and the secreted enzymes were assayed by steady-state kinetics. The result was that only one amino acid, Asp-70, was found to be important for the function. When Asp-70 was mutated to Gly, the same mutation as in the naturally occurring atypical butyrylcholinesterase, the affinity for positively charged substrates and positively charged inhibitors decreased 5–30-fold. The Asp-70Gly mutant had another striking abnormality in that it was virtually devoid of the phenomenon of substrate activation by excess butyrylthiocholine. Mutants containing aromatic amino acids at the mouth of the gorge had increased binding affinity for propidium and fasciculin, but unaltered function, suggesting that aromatic amino acids are not important to the function of the peripheral anionic site of butyrylcholinesterase.

A three-dimensional X-ray crystal structure of zinc-substituted phosphotriesterase, organophosphorus pesticides which are inhibitors of BChE was reported (Zhan *et al.*, 2003). It is uncertain whether a critical bridging ligand in the active site is a water molecule or a hydroxide ion. The identity of this bridging ligand is theoretically determined by performing both molecular dynamics simulations and quantum mechanical calculations. All of the results obtained indicate that this critical ligand in the active site of the reported X-ray crystal structure is a hydroxide anion rather than a water molecule and allow us to propose a dynamic "ping-pong" model in which both kinds of structures might exist. The kinetic data published on phosphotriesterase (PTE), with various complexed metals, (Koca *et al.*, 2001) indicated that the P=O and P=S bonds of phosphotriester and thiophosphotriester substrates, respectively, are polarized by one or both of the active site complexed metal ions. However, this observation is not consistent with the three-dimensional X-ray crystal structure of zinc-substituted PTE with active site bound substrate analogue diethyl 4-methylbenzylphosphonate. In their structure, the distance between the phosphoryl oxygen and the nearest zinc is 3.4 Å, a distance too large to afford strong polarization. In their work, the geometry and mobility of various PTE active site-substrate complexes were examined by performing both molecular dynamics (MD) simulations and quantum

mechanical calculations. The results indicated that PTE forms a complex with either substrate in which the phosphoryl oxygen becomes strongly coordinated with the less buried zinc atom. It is shown that the geometry of the active site is changed when the protein is immersed in a water bath and relaxed by MD.

Their reaction coordinate calcaulations support a double proton transfer mechanism and are against a single proton trasfer mechansim, as discussed from other works, (Hu *et al.*, 1998) presented results from QM calculations of the mechanism for serine hydrolase catalyzed ester hydrolysis. A model system containing both the catalytic triad and oxyanion hole was studied. The catalytic triad was represented by formate anion, imidazole, and methanol. The oxyanion hole was represented by two water molecules. Methyl formate was used as the substrate. They examined both single and double proton transfer mechanisms for the first step of acylation. The double-proton-transfer mechanism is unfavorable by about 2 kcal/mol. The bonds between the Asp group and the His group, and the hydrogen bonds in the oxyanion hole, increase in strength going from the Michaelis complex toward the transition state and the tetrahedral intermediate.

The describing semiempirical molecular orbital calculations of serine protease catalyzed hydrolysis of amides and esters (Daggett *et al.*, 1991), who found that attack of the substrate by the active site serine formed the tetrahedral, the intermediate was the rate-limiting step with both substrates. The lowest energy path for formation of the tetrahedral intermediate was for Ser to approach the substrate, followed by coupled heavy atom movement and proton transfer to complete the reaction. The effect of the environment on catalysis was estimated by calculating molecular mechanical interaction energies in both a noncovalent trypsin-peptide complex and a model for the transition state in which a covalent bond is imposed between O of the serine and the carbonyl carbon of the substrate. It was found that the environment itself was important in stabilizing the transition state compared to the Michaelis complex in addition to

stabilization by the asparatic acid of the catalytic triad and the oxyanion hole.

The absolute activation barriers reported from the PM3 study (Hwang and Warshel, 1987) gave an estimated error of about 5 kcal/mol. Using longer simulation time in a study of the catalytic reaction of trypsin reproduced the observed change in $\Delta G'$, but this could reflect an accidental success. The present study, however, has examined additional test cases and reproduced the observed change in $\Delta G'$ to within 1 kcal/mol. This might mean that we are entering a stage of quantitative structure function correlation in macromolecules. Hwang and Warshel (1987)'s work indicates that the changes in catalytic free energies can be estimated by calculating the electrostatic energy (solvation energy) of the *charges* of the relevant resonance structures. This reinforces the idea that enzymes can be viewed as "supersolvents" for the charges during the reaction and that the evaluation of the solvation energy of the reacting substrate by the enzyme-water system is the key for understanding enzyme catalysis.

The double-proton transfer mechanism for serine hydrolase hydrolysis has been studied, although some experiments and EVB simulations have been carried out for this mechanism (Warshel and Ressell, 1986; Sholten *et al.*, 1988). The mechanism involves a proton transfer from Ser to His and a proton transfer from His to Asp at the tetrahedral intermediate.

There have been suggestions that strong, low-barrier hydrogen bonds (LBHBs) play an important role in serine protease (Gerlt and Gassman, 1993). They proposed that the rates of enzyme-catalyzed abstraction of protons from carbons adjacent to carbonyl or carboxylic acid groups could be understood if proton abstraction by an active site general basic catalyst was concerted with protonation of the carbonyl group by an active site general acidic (electrophilic) catalyst to generate an enol intermediate instead of an enolate anion (aldehyde, ketone, or thioester substrate) or dianion (carboxylic acid substrate. They analyzed concerted general acid-general base catalyzed enolization

reactions in terms of Marcus formalism that partitions the activation energy barrier for the reaction, AG*, into (1) a thermodynamic component, $\Delta G°$, associated with both the conversion of the keto tautomer of the carbon acid into its enol tautomer and the transfer of a proton from the general acidic catalyst to the general basic catalyst, and (2), an intrinsic kinetic component, AG*int, for the activation energy for the reaction in the absence of a thermodynamic barrier,. they propose that in enzyme active sites both $\Delta G°$ and AG*int are reduced from the values that describe nonenzymatic reactions. The transition states for the enzymatic reactions are "late", i.e., the transition states resemble the enol tautomers of the substrate carbon acids, as suggested by the observation that the pKas of the OH groups of the enols are similar to the pK,s of the uncharged active site general acidic catalysts. The late transition states in enzyme-catalyzed reactions can be explained best by reductions in AG*int from the values that describe nonenzymatic reactions (Frey *et al.*, 1994; Cleland and Kreevoy, 1994; Golubev *et al.*, 1994).

Although there have been debates over the hypothesis that LBHBs facilitate the catalytic function of the enzyme in many works (Cleland and Kreevoy, 1994; Warshel *et al.* 1995; Frey, 1995; Warshel and Papazyan, 1996), the existence of very strong hydrogen bonds in the action of enzyme is an attractive feature. According to the study, Ab initio calculations are used to test a recent suggestion that enzymic catalysis can be aided by the strengthening of a hydrogen bond in a key intermediate, occurring when this bond is shortened and the pKa's of the two groups are equalized (Scheiner and Kar, 1995). The requisite amount of energy is not available in electrically neutral H-bonds; no additional strengthening can be accomplished by shortening such a bond. Interaction energies where one subunit is charged, on the other hand, can be very high. These bonds are intrinsically very short, and the proton transfer profile contains a very low energy barrier. There is no special stabilization associated with the disappearance of the transfer barrier or equalization of the pKa's.

A number of theoretical studies have shown that hydrogen bonds are largely

electrostatic in nature (Warshel *et al.,* 1996; Murray *et al.,* 1991; Murray *et al.,* 1992; Murray and Politzer, 1994; Hagelin *et al.,* 1995; Kollman, 1981; Dinur and Hagler, 1991; Brinck *et al.,* 1993). Although the hydrogen bonds in this work are strong and are expected to have a significant degree of covalent character, the increase in the hydrogen bond strengths is from ES1 to TS1 and to INT1. The catalytic activity of the catalytic triad and the oxyanion hole can be explained from electrostatic considerations. The transfer of the O1H1 of Ser-198 to N1 of His-438 leads to a charge separation of the system which results in a large positive electrostatic potential on the His-438 proton that binds Glu-325. The increase of the hydrogen bond strength in the oxyanion hole can also be said to be a consequence of an increased electrostatic interaction. It can further be said that the catalytic activity of an enzyme seems to be an effect of an increased electrostatic stabilization of the hydrogen bonds in TS1 compared to ES. Warshell and Ressell (1986) and Warshell *et al.* (1989) have concluded that serine protease works by electrostatic stabilization of the transition state.

Other theoretical calculations of cocaine hydrolysis, MNDO, AM1, PM3 and SM3 semiempirical molecular orbital methods, as well as an ab initio procedure at the HF/3-21G level of theory were employed to optimize geometries of the transition states for the frist step of the hydrolysis of cocaine and model esters, including methyl acetate, were studied (Sherer *et al.*, 1995; Turner and Sherer, 1995). Then, the use of density functional theory was used to examine the energy barriers for the alkaline hydrolysis of the cocaine benzoyl-ester (Zhan *et al.*, 2001). The reaction coordinate calculations indicate that the mechanism is two steps. The first step is the formation of a tetrahedral intermediate for the energy barrier, 7.6 kcal/mol, which is 4 kcal/mol lower than that for $CH_3C(O)OCH_3$ hydrolysis (11.4 kcal/mol) calculated at the same level, which is in agreement with the experimental data, 12.2 kcal/mol (Rylander and Tarbell, 1950) and 10.45 kcal/mol was calculated (Fairclough and Hinshelwood, 1937).

Many works have also studied various aspects of the reactions catalyzed by AChE and BChE. The accounction for protein dynamics and investigation of the effect of

different conformations on the enzyme reaction energy barrier. The initial step of the acylation reaction catalyzed by acetylcholinesterase (AChE) with a multiple QM/MM reaction path approach was considered (Zhang *et al.*, 2003). The approach consists of two main components: generating enzyme-substrate conformations with classical molecular dynamics simulation and mapping out the minimum reaction energy path for each conformational snapshot with combined quantum mechanical/molecular mechanical (QM/MM) calculations. It was found that enzyme-substrate conformation fluctuations lead to significant differences in the calculated reaction energy barrier; however, the qualitative picture of the role of the catalytic triad and oxyanion hole in AChE catalysis is very consistent. Their results emphasized the importance of employing multiple starting structures in the QM/MM study of enzyme reactions and indicated that structural fluctuation is an integral part of the enzyme reaction process.

Then, the calculation of the geometries of the transition states, intermediates, and prereactive enzyme-substrate complex and the corresponding energy barriers have been determined by performing hybrid quantum mechanical/molecular mechanical (QM/MM) calculations on butyrylcholinesterase (BChE)-catalyzed hydrolysis of (−)- and (+)- cocaine (Zhan and Gao, 2005). The energy barriers were evaluated by performing QM/MM calculations with the QM method at the MP2/6-31+G* level and the MM method using the AMBER force field. These calculations allow accounting for the protein environmental effects on the transition states and energy barriers of these enzymatic reactions, showing remarkable effects of the protein environment on intermolecular hydrogen bonding (with an oxyanion hole), which is crucial for the transition state stabilization and, therefore, on the energy barriers. The calculated energy barriers are consistent with available experimental kinetic data. The highest barrier calculated for BChE-catalyzed hydrolysis of (−)- and (+)-cocaine is associated with the third reaction step, but the energy barrier calculated for the first step is close to the highest and is so sensitive to the protein environment that the first reaction step can be rate determining for (−)-cocaine hydrolysis catalyzed by a BChE mutant. The computational results provided

valuable insights into future design of BChE mutants with a higher catalytic activity for (−)-cocaine.

The reaction pathways for the alkaline hydrolysis of carboxylic acid esters, RCOOR′, were examined through a series of first-principle calculations. The reactions of six representative esters with hydroxide ion were studied in the gas phase. A total of three competing reaction pathways were found and theoretically confirmed for each of the esters examined: bimolecular base-catalyzed acyl-oxygen cleavage (BAC2), bimolecular base-catalyzed alkyl-oxygen cleavage (BAL2), and carbonyl oxygen exchange with hydroxide. For the two-step BAC2 process, this is the first theoretical study to consider the individual sub-steps of the reaction process and to consider substituent effects. For the carbonyl oxygen exchange with hydroxide and for the one-step BAL2 process (Zhan *et al.*, 2000). They reported the first quantitative theoretical results for the reaction pathways and for the energy barriers. The calculated substituent shifts of the energy barrier for the first step of the BAC2 process in the gas phase are in good agreement with the observed substituent shifts for the base-catalyzed hydrolysis of alkyl acetates in aqueous solution. All of the calculated results are consistent with the available experimental results and lead to a deeper understanding of previously reported gas-phase experimental observations.

Additionally, an investigation of a series of ab initio molecular orbital and density functional theory calculations was performed to examine the reaction pathways and the corresponding energy barriers for the alkaline hydrolysis of the cocaine benzoyl-ester and methyl-ester groups and three model esters in aqueous solution (Zhan and Landry, 2001). The reaction coordinate calculations indicated that the mechanisms of the base-catalyzed hydrolysis of both the benzoyl-ester and methyl-ester groups of neutral cocaine were similar to the usual two-step BAC2 route of hydrolysis of alkyl esters. The first step is the formation of a tetrahedral intermediate by the attack of hydroxide oxygen at the carbonyl carbon of the cocaine methyl-ester or benzoylester. The second step is the decomposition of the tetrahedral intermediate to products. The solvation calculations

revealed the importance of the solvent effects on the energy barriers and indicated that the extremely large solvent shifts of the energy barriers for the first step of the ester hydrolysis are attributed mainly to the contributions of the long-range solute-solvent electrostatic interactions.

The solvent effects and energy barriers have been determined for the base-catalyzed hydrolysis of two representative alkyl esters in aqueous solution, using a hybrid supermolecule-polarizable continuum approach (Zhan *et al.*, 2000). Four solvent water molecules were explicitly included in the supermolecular reaction coordinate calculations. Two competing reaction pathways were investigated. The first pathway involves a direct proton transfer in the second step which is the decomposition of the tetrahedral intermediate. The second pathway involves a water-assisted proton transfer during the decomposition of the tetrahedral intermediate. The direct participation of the solvent water molecule in the proton-transfer process significantly drops the energy barrier for the decomposition of the tetrahedral intermediate. Thus, the energy barrier calculated for the decomposition of the tetrahedral intermediate through the water-assisted proton transfer becomes lower than the barrier for the formation of the tetrahedral intermediate, while the direct proton transfer is higher. The favorable pathway involves water-assisted proton transfer and the energy barriers are calculated using the hybrid supermolecule-polarizable continuum approach.

Also, the study of five different SCRF procedures were employed to evaluate the energy barriers for both the BAC2 and BAL2 modes of hydrolysis of six representative alkyl esters in aqueous solution (Zhan *et al.*, 2000). The calculated results revealed that electron correlation effects on the solvent shifts of the energy barriers determined by the SVPE and SPE calculations are all very small. The differences between the solvent shifts calculated at the HF/6-31++G(d,p) level and those at the MP2/6-31++G(d,p) level are only 0.0-0.3 kcal/mol. The differences become slightly larger for the solvent shifts of the energy barriers determined by the other SCRF calculations in which the cavity surface is

defined as the overlapped spheres. The calculated results indicate the basis for the observation that in aqueous solution the BAL2 process is negligible compared to the corresponding BAC2 process, although both the BAC2 and BAL2 hydrolyses of methyl esters are competitive in the gas phase.

Another type of cholinesterase is actylcholinesterase. The calculated initial step of the acylation reaction catalyzed by acetylcholinesterase (AChE) by a combined ab initio quantum mechanical/molecular mechanical (QM/MM) approach. The reaction proceeds through the nucleophilic addition of the Ser-203 O to the carbonyl C of acetylcholine, and the reaction is facilitated by simultaneous proton transfer from Ser-203 to His-447. The calculated potential energy barrier at the MP2(6-31+G*) QM/MM level is 10.5 kcal/mol, consistent with the experimental reaction rate. The third residue of the catalytic triad, Glu-334, is found to be essential in stabilizing the transition state through electrostatic interactions. The oxyanion hole, formed by peptidic NH groups from Gly-121, Gly-122, and Ala-204, is also found to play an important role in catalysis. The calculations indicated that, in the AChEACh Michaelis complex, only two hydrogen bonds are formed between the carbonyl oxygen of ACh and the peptidic NH groups of Gly-121 and Gly-122. As the reaction proceeds, the distance between the carbonyl oxygen of ACh and NH group of Ala-204 becomes smaller, and the third hydrogen bond is formed both in the transition state and in the tetrahedral intermediate (Zhang *et al.*, 2002).

The energetics of the acylation step of AChE (acetylcholinesterase) is explored by using molecular simulation approaches (Fuxreiter and Warshel, 1998). These include the evaluation of activation free energies by using the empirical valence bond (EVB) potential surface and an all-atom free energy perturbation (FEP) approach, as well as estimates of the catalytic effect of the enzyme by using the semimicroscopic version of the Protein Dipoles Langevin Dipoles (PDLD/S) method. The determination of the effect of the enzyme is based on the use of reliable experimental information in evaluating the

energetics of the reference reaction in water and then on using robust simulations for the evaluation of the effect of moving the reacting system from a solvent cage to the protein active site. Both the EVB and PDLD/S approaches show that the enzyme reduces the activation barrier of the acylation step by 10-15 kcal/mol relative to the corresponding reference reaction in water. This corresponds to a (107-1011)-fold rate acceleration, which is in good agreement with the corresponding experimental estimate. The origin of the catalytic power of the enzyme appears to be associated with the electrostatic stabilization of the transition state. This electrostatic effect can be classified as a combination of reduction of the energy of the charged intermediate and reduction in the reorganization energy. The contributions of different protein residues to the stabilization of the transition state are estimated. It is demonstrated that, in contrast to some proposals, AChE and other enzymes do not work by providing a hydrophobic environment but rather a polar environment.

Moreover, The deacylation step of acetylcholinesterase was simulated using the empirical valence bond (EVB) method in combination with free energy perturbation calculations (Knapp *et al.*, 2000). Before the enzyme structure was used to simulate the reaction, the protonation pattern of the acylated enzyme and the free enzyme was determined by a Monte Carlo titration. As a result, they found that Glu-199, which is located close to the catalytic triad, is protonated in the free and acylated enzyme. Also, the EVB simulation of the reaction showed that the uncharged Glu-199 is favorable to stabilize the transition state of the deacylation step. This is in agreement with experiments demonstrating that the Glu-199Gln mutation does not have a significant influence on the kinetics of deacylation. The EVB calculations yielded an energy barrier of the deacylation step that is 11-12 kcal/mol lower in AChE as compared to a reference reaction in water. The largest calculated rate of the deacylation reaction is $k_{cat} = 5.5 \times 10^2 \text{ s}^{-1}$ and thus, only by a factor of 30, smaller than the experimental value.

The 3D model of BChE was constructed by the comparative modeling technique and using the program MODELLER to develop the model. BChE has a similar channel

as AChE leading to the active site, 5 Å wider than the active site in AChE. Also, it did not contain as many aromatic amino acids. A minor difference is that the space of the active site in BChE is greater than that in AChE. An intra-aromatic distance analysis of the active site indicates that two hydrogen bonds easily form in AChE, but only one in BChE. The active site in AChE is more rigid, not allowing the substrate to move as freely as in BChE (Ekholm and Konschin, 1999).

Also, there is the prediction that the Michaelis-Menten complexes of BChE liganded with natural and unnatural cocaine molecules by molecular dynamics (MD) simulations. Both (+)-cocaine and (-)-cocaine isomers need to rotate their benzoic ester group toward the catalytic Ser-198 for hydrolysis. On the basis of the 3D models, they predicted that rotation of (+)-cocaine would be rapid and that the rate-limiting step in hydrolysis would involve acylation. Thus hydrolysis of (+)-cocaine would be expected to be heavily influenced by pH. They also predicted that rotation of (-)-cocaine would be hindered by pi-pi interaction involving its phenyl ring and that the rate-limiting step in hydrolysis would be determined mainly by the rate of substrate reorientation. Thus, hydrolysis of (-)-cocaine would be less pH-sensitive. Experimental studies confirmed both of these predictions (Sun *et al.*, 2001).

Other literatures provide a detailed mechanism of BChE and cocaine. Harel *et al.*, (1992) constructed a computer-based model of BChE from the x-ray crystal structure of *Torpedo california* AChE. Also, other works have reported similar models (Millard and Broomfield, 1992; Millard *et al.*, 1995; Millard *et al.*, 1998; Masson *et al.*, 1997; Berkman *et al.*, 1997; Xie *et al.*, 1999; and Saxena *et al.*, 1997).

The role of Glu-325 in the catalytic triad is still questionable. Suggestions have been made in many literatures, (Warshel *et al.*, 1986; Warshel *et al.*, 1989; Fuxreiter *et al.*, 1998). They suggested that the electrostatic interaction between the carboylate of Glu-325 and the incipient imidazolium cation stabilizes the transition state and the

tetrahedral intermediate.

Secondly it was suggested that it is a charge-relay mechanism, the carboxylate of Glu-325 being like a general acid-base catalyst. It is involved in the proton transfer between His-438 and Glu-325 (Blow *et al*., 1969; Bachovchin *et al.*, 1978).

Finally, it has been suggested that the low-barrier hydrogen bond mechanism, which the low-barrier hydrogen bond formed between carboxylate of Glu-325 and the imidazolium cation of His-438, stabilizes energy to lower the reaction barrier (Massiah *et al.*, 2001).

A similar study of the role of Glu-325 has explored the empirical valence bond (EVB) approach used in correlation to the catalytic activity of trypsin. It indicated that the most important interaction in the catalytic triad of serine proteases is the stabilization of the negative charge tetrahedral intermediate by the main-chain N-H of the "oxyanion hole" and binding with water molecules. An analysis of the popular "charge-relay" mechanism indicated that this mechanism is unlikely to be important for the catalytic activity of serine proteases; apparently a transfer of a proton from His-57 to Asp-102 involved an increase of the energy of the transition state by about 10 kcal/mol (Warshel and Ressell, 1986).

On the basis of kinetic data and molecular-modeling results, it has been proposed that the peculiar kinetic properties of BChE are most likely induced by excess substrate molecules bound to the so-called "peripheral" and "intermediate" sites, whose existence has been confirmed by the X-ray structures of BChE complexed with butyrylcholine or soman (Nicholet *et al.*, 2003). The peripheral site is located at the rim of the aromatic gorge and contains the residue Asp-70, which presumably plays an important role in stabilizing and orienting the excess substrate molecules. The intermediate site is located near the bottom of the gorge channel, where the indole group of Trp-82 interacts with the

positively charged choline head of substrate molecules to give a cation-π complex. It must be noted that the subtle molecular details through which the excess substrate molecule bound to the catalytic cavity remain to be elucidated.

Other features of cholinesterasses manifested in their crystallographic structures are: (a) their ability to bind neutral molecules (polyethylene gylcol and glycerol), at the cation recognition site through interactions that structurally mimic the cation-π interactions formed in substrate binding; and (b) the presence of electron-density peaks very close to the catalytic Ser residue that can be modeled as small anionic molecules (carbonate and sulfate). In addition, in the electron-density peak adjacent to the Ser-198 residues was best modeled as a tetrahedral butyryl group bound to Ser-198 with a Ser-198 O to C butyryl distance of 2.16 Å (Harel *et al.*, 2000; Bourne *et al.*, 2003).

Several lines of evidence confirm this interpretation because further experimental work has shown that: (a) 3-bromopropionate, when used to replace butyrate, is found in this position; (b) the moiety is displaced by choline; and (c) the presence of butyrate turned out to be essential for crystrallization because butyrate-depleted BChE samples are extremely difficult to crystallize. The presence of a putative butyrate bound to Ser-198 is also sterically compatible with substrate binding at the intermediate site by analysis of the X-ray structure of the soman-aged BChE-BTC complex. All of these results suggest that binding of butyrate to the Ser-198 hydroxyl group could be somehow related to the resistivity and/or stability of the catalytic serine. Hence, it has been proposed that concerted product release/substrate binding at a depronated Ser-198 could be a mechanisitc alternative to the expected activation of Ser-198 by the nearby His-438 (Nicholet *et al.*, 2003).

The investigation of the mechanism of the deacylation step in the active site human butyrylcholinesterase (Suarez *et al.*, 2006) was carried out by quantum mechanical (QM) calculations on cluster models of the active site built from a

crystalllographic structure. Analyses of the equilibrium geometries, electronic properties and energies of the QM models gave insights into the catalytic mechanism. In addition, the QM calculations provided the data required to build a molecular mechanics representation of the reactive BChE region that was employed in molecular dynamics (MD) simulations followed by molecular-mechanics-Poisson-Boltzmann (MM-PB) calculations. The presence of glycerol or butyrylcholine stabilizes a product complex formed between a butyric acid molecule and BChE. Their results agreed with the crystallographic structure of BChE, in which the catalytic Ser-198 interacts with a butyric fragment, while the cation-π site is occupied by a glycerol molecule.

Studies of long-range electrostatic interaction of the zeolite lattice were proposed by Lomratsiri *et al.*, (2006) using the model called "embedded ONIOM". The adsorption energy at B3LYP/6-31G(d,p) level is in excellent agreement with the experimental value. Also, a similar work studied the cumene formation via benzene alkylation with propylene on the new three-dimensional nanoporous catalyst, ITQ-24 zeolite using the ONIOM2(B3LYP/6-31G(d,p):UFF) method. The contributions of the short-range van der Waals interactions, which are explicitly included in the ONIOM2 model, and an additional long-range electrostatic potential from the extended zeolite framework to the energy profile are taken into consideration (Jangsang *et al.,* 2006). Finally, there was the proposal of a simple method for including this effect into the calculation by generating a finite number of point charges placed upon the lattice sites. These point charges reproduce the infinite electrostatic potential at the chemically important region of the zeolite (Injan *et al.*, 2005). They applied this method to the adsorption of pyridine on H-Faujasite zeolite and compared it with calculations without including the field effect. The embedding method gave an adsorption energy of 42.8 kcal/mol, which agrees well with the experimental value of 43.1±1 kcal/mol. Without the electrostatic effect of the crystal field, the value is about 9 kcal/mol higher.

METHODS OF CALCULATIONS

1. Implicit solvent model

There are many approaches to approximate solvent effects in molecular dynamics, some of which will be demonstrated in this section. This approach does not consider the solvent effect as an explicit effect, so the calculation is called *implicit solvent models*. The interaction between the solvent and solute is described as a function of the solute coordinates. All effects of the solvent, such as polar screening of charges, and van der Waals interaction cavitations, are accounted for by the appropriate functions. The effective energy function of the macromolecule that consists of intramolecule interactions and solvent-molecue coupling terms is shown below in the form:

$$W(\vec{r}_i M) = H_{mm}(\vec{r}_i M) + DG_{solv}(\vec{r}_i M) \qquad (3.1)$$

Where the molecule consists of M atoms in the Cartesian coordinates $\vec{r}_i = (\vec{x}_i, \vec{y}_i, \vec{z}_i)$ where $i = 1, ..., M$. The solvation energy term D$g$solv is divided into three terms. The first term is the cavitation, which is the rearrangement of the solvent molecules around the solute. The second term is the hydrophobicity, which is that the interactions come from the polar solvent to avoid being too close to the non-polar sides of the protein. The last term is the electrostatic solvation contribution, which is the shielding effect of the polarization of the solvent of the electrostatic interaction. The first two terms have entrophy and enthalpy contributions, while the last term, demonstrated in the models discussed in this section, has only enthalpy contributions.

An implicit solvent method in molecular dynamics significantly reduces computational time because the number of degrees of freedom is decreased by one order of magnitude. Furthermore, the equilibrium of solvent induced by large conformational changes in the solute, like folding or unfolding, occurs simultaneously. In respect of the

molecular dynamics simulation, the solvation free energy is changed in each step by the change in the solute coordinates. This suggests that solvent and solute is in thermodynamic equilibrium immediately. The rearrangement of explicit solvent molecules slows to give a significant result: solvent-solute interactions need to be averaged for a long time in order to provide meaningul results (Feig and Brook, 1998). So, the conformational transitions are studied by molecular dynamics, and the use of implicit solvents have advantages. An implicit solvent provides a more efficient sample by the reduction of solvent-solute interactions to mean field interactions.

In many cases, the solvent-solute interaction is described as the most important (Levy and Gallicchio, 1998), for example in the simulation of hydrogen bonds. Since the explicit solvent model is needed, the implicit solvent models cannot account for specific solvent-solute hydrogen bond interactions.

In the next section, the continuum, Poisson-Boltzmann formalism and the generalized Born approximation are presented.

2. Poisson-Boltzmann equation

The exact explanation of electrostatic interactions in a continuum dielectric medium is provided by the Poisson equation. If some charge distribution $\rho(r)$ is in an environment, it will have the regular dielectric constant ε, and the electrostatic potential $\phi(r)$. The equation is:

$$\Delta\phi(\vec{r}) = -4\pi\frac{\rho(\vec{r})}{\varepsilon}$$

If the dielectric medium is nonhomogeneous, that is the dielectric constant depends on the position, $\varepsilon = \varepsilon(r)$, the equation is generalized as:

$$\nabla \cdot [\varepsilon(\vec{r})\nabla\Phi(\vec{r})] = -4\pi\rho(\vec{r})$$

In the simple case of dielectric constant ε, the solution of the Poisson equation is better known as the Coulomb potential:

$$\phi(\vec{r}) = \int_{v} \frac{\rho(\vec{r}')d\vec{r}'}{\varepsilon|\vec{r} - \vec{r}'|}$$

A protein can represent a set of point charges for each atom that is distributed in a low dielectric medium. The solvent around the solute is given by a high dielectric constant medium and contains:
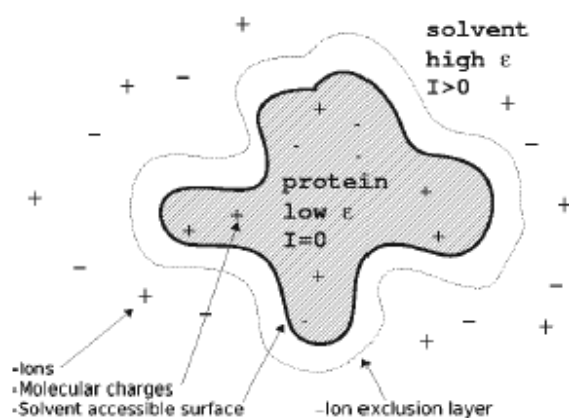
Figure 5 Sketch of a molecule embedded in an ionic solution, according to the continuum representation (Rabenstein, 2000).

One can write a Poisson equation for protein, where the charge distribution $\rho(r)$ is the sum of delta functions that are represented as point charges. The dielectric function is given two different values and is divided into two regions by protein surface, one is called a 'low values in protein interior', as 2 or 4, and the other, a 'high values in aqueous solution', which is close to 80. The accurate value of ε in the solute is not clear (Warshell *et al.,*1997; Ullmann and Knapp, 1999; Rabenstein *et al.,* 1998). To obtain a real description of solvated protein, ions in solution surrounding the molecule are needed. Their effect includes the use of ion distribution which results from a Boltzmann statistics in an approximately mean field. The equation for this is:

$$\rho_{ion}(\vec{r}) = \sum_{s} c_s(\vec{r}) q_s \exp(-\beta q_s \phi(\vec{r}))$$

where s is the number present in the species

   c_s is the local concentration of species s

   q_s is charge of species s

The Boltzmann constant is given by $\beta = 1/k_B T$

So, the following Poisson-Boltzmann equation is obtained:

$$\nabla \cdot [\varepsilon(\vec{r}) \nabla \phi(\vec{r})] = -4\pi [\rho(\vec{r}) + \rho_{ion}]$$

$$= -4\pi \rho(\vec{r}) - 4\pi \sum_{s} c_s(\vec{r}) q_s \exp(-\beta q_s \phi(\vec{r}))$$

A linear version of the Poisson-Boltzmann equation can be written by expanding the exponential as the power series in the electrostatic contributions (up to the first order):

$$\sum_{s} c_s(\vec{r}) q_s \exp(-\beta q_s \phi(\vec{r})) = \sum_{s} c_s(\vec{r}) q_s - \beta \sum_{s} c_s(\vec{r}) q_s^2 \phi(\vec{r}) + ...$$

The term of order zero will disappear through the hypothesis of electroneutrality of the ionic solution:

◘

$$\sum_s c_s(\vec{r})q_s = 0$$

such that the linear Poisson-Boltzmann equation (LPBE) becomes:

$$\nabla \cdot [\varepsilon(\vec{r})\nabla\phi(\vec{r})] - 8\pi I(\vec{r}) = -4\pi\rho(\vec{r})$$

using the definition of the ionic strength *I(r)*:

$$I(\vec{r}) = \frac{1}{2}\sum_s c_s(\vec{r})q_s^2$$

3. Computational Method

Molecular modeling is an essential tool for understanding molecular properties. Computer calculation enables the calculation of molecular geometries, energies and physical properties with varying degrees of accuracy, depending on the calculation method and on the level of the theory. Some of the modeling methods are discussed in this chapter.

Three different models have been employed to study this reaction pathway. First, the quantum cluster model was taken from the active site of a three-dimensional model of human BChE as constructed by Harel *et al.,* (1992). Other works have reported an application with other substrates (Millard *et al.,* 1992; Sun *et al.,* 2001; Ekholm *et al.,* 1999; Saxena *et al.,* 1997; Masson *et al.,* 1999).

Our quantum cluster model contains both the catalytic triad and the oxyanion hole as well as the cocaine substrate molecule. The catalytic triad consists of Ser198, His437 and Glu325, represented by methanol, imidazole and acetate. The oxyanion hole, which is the enzymatic active site that can form peptidic hydrogen bonds with carbonyl oxygen of cocaine, consists of Glu116, Glu117 and Ala199 residues, represented by two glutamine amino acids and an alanine amino acid. The enzyme-substrate complex of BChE and cocaine is illustrated in Figure 6.

For computational efficiency, only the small active region is treated quantum mechanically with the density functinal theory method, while the contribution of interactions from the rest of the model is taken into account by using a less computationally expensive embedding quantum cluster scheme. The B3LYP/6-31G(d,p) level of theory was applied to evaluate the catalytic activity of the enzyme-substrate complex. All calculations were performed on a Linux workstation using the Gaussian 03 program (Frisch *et al.,* 2001). During the optimization, the enzymatic active site and the

cocaine substrate were permitted to relax while the terminated hydrogen atoms of Ser-198, His-437 and Glu-325 were fixed along the original crystallographic bond directions. The frequency calculations were performed at the same level of theory to ensure that an obtained transition state structure has only one imaginary frequency that corresponds to a saddle point of the required reaction coordinate.

In order to take into account the long-range interactions of the enzyme framework, a second model, called "electronic embedding scheme," is employed (Fig. 7). This model consists of two layers: the inner layer, which is the active site region, is treated quantum mechanically; the outer layer of the model, extended from the active site, is made up of two sets of point charges, explicit charges and optimized charges, is to reproduce the medium- and long-range effects of the electrostatic Madelung potential from the enzyme framework (Dungsrikaew *et al.,* 2003; Injan *et al.,* 2005). The explicit charges generated by the AMBER program are placed at the crystallographic atomic positions of the enzyme framework within a cutoff radius of 12 Å from the center of the quantum cluster. The second set consists of point charges placed upon crystallographic coordinates (Figures 7a-d) to reproduce the long-range electrostatic field from the extended enzyme framework. Using two sets of point charges in such a way can be developed in studies of several enzyme systems.

Also, the solvation effect on the energy barriers of this pathway were studied by a continuum model that takes into account the nonspecific solute-solvent interaction, using the reaction field formalism. The solvent is considered as a polarization continuous dielectric medium, characterized by a dielectric constant ε, and the solute is imbedded inside a cavity in the continuum. In this study, the self-consistent reaction field (SCRF) method based on Gauss's Law for the exact solution of Poisson's equation (Tomasi *et al.,* 1994; Cramer *et al.,* 1999; Chipman *et al.,* 1997; Chipman *et al.,* 1999; Chipman *et al.,* 2000) was employed by the polarized continuum model (PCM) (Miertus *et al.,* 1981; Miertus *et al.,* 1982; Cossi *et al.,*1996) calculated for the continuum-based calculations.

To investigate solvation effects, the PCM single-point energy calculations in aqueous ($\varepsilon = 78.4$) solution were imposed on the optimized quantum cluster models computed at the B3LYP/6-31G(d,p) level of theory.

(a)

(b)
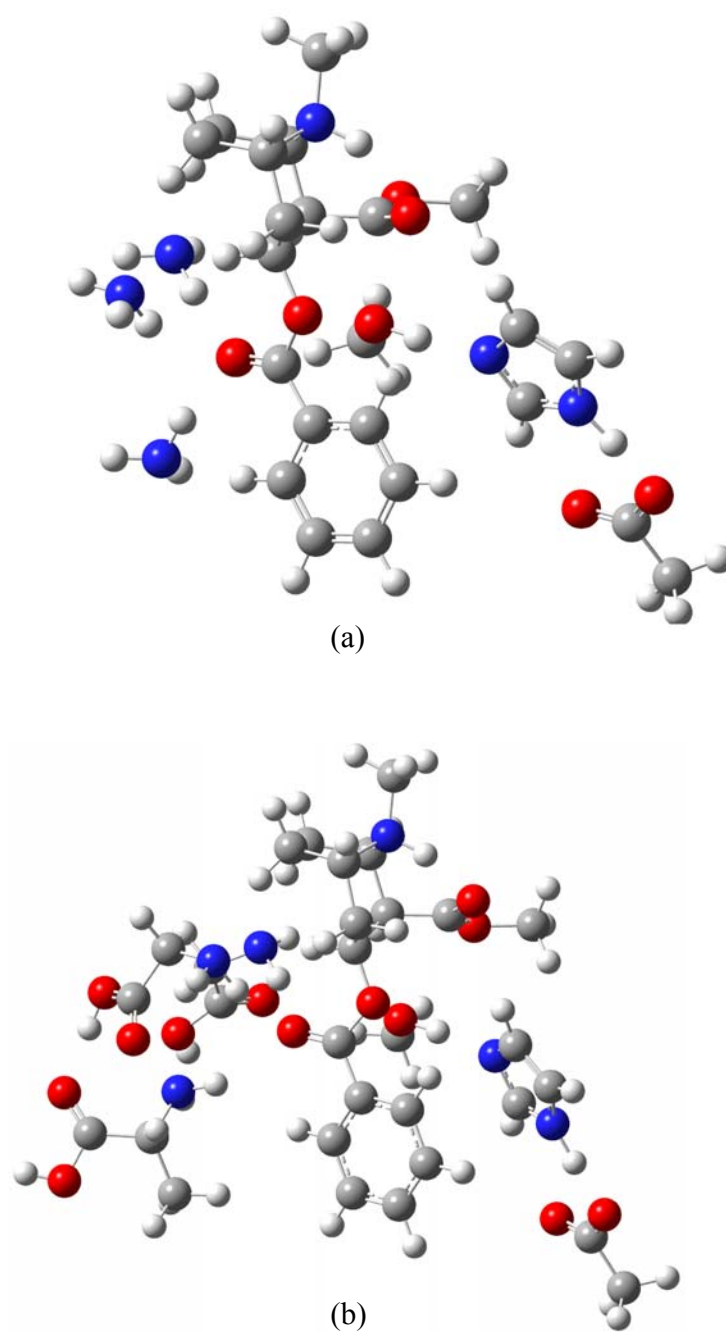
Figure 6 Structure of Cluster (a) and Cluster-amino acid (b) model of
butyrylcholinesterase
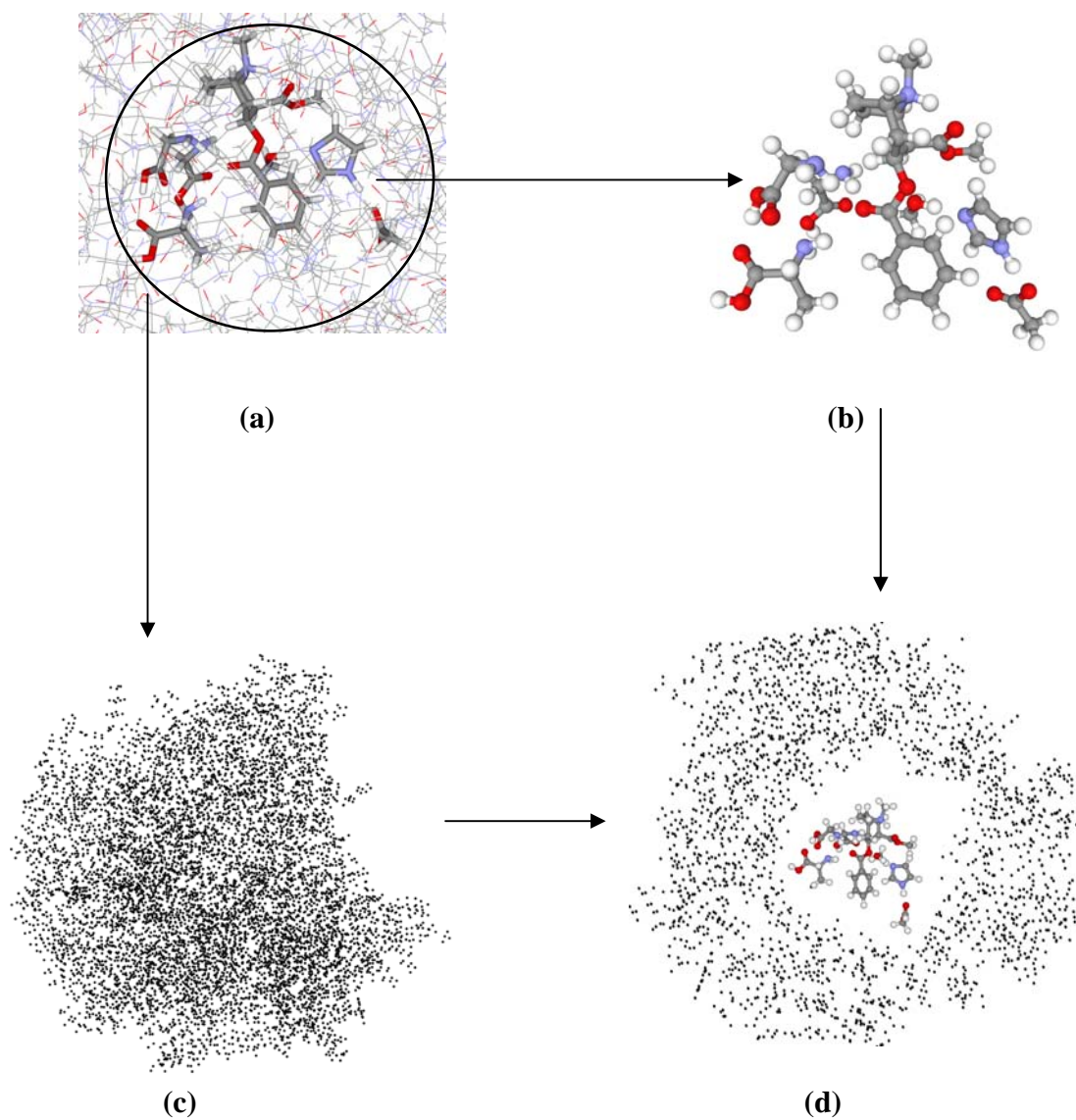
Figure 7 Schematic diagram for electronic embedding method. The framework of structure of BChE (a) was divided into two layers: the inner layer is the QM region (b); the outer layer is a set of point charges (c). The complete electronic embedding model is shown in (d).

RESULTS AND DISCUSSION

The schematic representation for the acylation step of the cocaine-BChE hydrolase catalysis is illustrated in Scheme 1. To compare this with previous theoretical calculations, the starting configuration of the BChE-cocaine complex model was taken from the fully optimized structure by the MD simulations to minimize structures of BChE binding with cocaine (Zhan *et al.,* 2003), the internuclear distance between the carbonyl carbon of the benzoyl ester of cocaine and O1 Ser-198 is 3.19 Å. The C1-O1 distance compared to the distance between the carbonyl carbon and the hydroxide oxygen is 2.99-3.56 Å, the optimized geometries of the prereactive enzyme-substrate complex of carboxylic acid esters with hydroxide (Zhan *et al.,* 2000; Zhan and Landry, 2001). The distances between carbonyl oxygen O4 of the benzoyl ester of cocaine and the NH of three-pronged oxyaniom hole (Gly-116, Gly-117 and Ala-199) are 1.98, 2.59 and 1.92 Å, respectively.

This structure was reoptimized the cluster model in this work at the B3LYP/6-31G(d,p) level of theory in order to obtain more reliable geometry. The model consists of the catalytic triad Ser-198, His-438 and Glu-325, which are represented by methanol, imidazole and acetate, respectively, and the oxyanion hole Gly-116, Gly-117 and Ala-199 represented by three ammonia molecules. The converged geometry of the corresponding prereactive BChE-cocaine complex, which is referred to as the enzyme-substrate (ES) complex, is illustrated in Figure 8a. The cocaine molecule binds to the active site with an orientation in which a carbonyl oxygen can form weak H-bonds with the three-pronged oxyanion hole. At this configuration, the cocaine carbonyl carbon ($C_{carbonyl}$) is in the position that is reachable for the Ser-198 O^{γ} with the $C_{carbonyl}\cdots O1$ distance of 2.57 Å. The catalytic triad is energetically arranged by forming two H-bonds, i.e., between Ser-198 and His-438 and between His-438 and Glu-325 (Figures 2a, 3a and 4a). All selected structural parameters of the ES complex are tabulated in Table 1.

The acylation is initialized by the attack of the Ser-198 O^γ at the carbonyl carbon of cocaine benzyl ester group to form the first tetrahedral intermediate (INT1) through the first transition state (TS1) (Scheme 1 and Figures 9a and 9b)., The distances of O1-H1 and N2-H2 in the optimized structure in the ES-complex are 1.02 and 1.09 Å, respectively. In the TS1, the bond between the carbonyl carbon and Ser-198 O^γ ($C_{carbonyl}$···O1) is formed. The bond is decreased from that in ES1, 2.57 Å, to that in TS1, 2.17 Å, at the same time that H1 of the Ser-198 OH is being transferred to the imidazole N1 of His-438, the distance of O1-H1 is lengthened from ES1 to 1.22 Å. These events are concurrent with the migration of the imidazole H2 of His-438 to the carboxylate anion O2 of Glu-325, the length of N2-H2 bond increases 0.47 Å to 1.22 Å. The transfer of the O1H1 of Ser-198 to N1 of His-438 leads to a charge separation of the system which results in a large positive electrostatic potential on the His-438 proton that binds Glu-325. The increase of the hydrogen bond strength in the oxyanion hole can also be said to be a consequence of the increased electrostatic interaction. During the formation of INT1, the C1-O1 bond, which is shortened to 1.33 Å, is already formed. While The distance of O1-H1 and H1-N1 bond is 3.44 and 1.12 Å, respectively, and that of the N2-H2 bond is 1.59 Å. It shows that H1 of the Ser-198 OH and H2 of the imidazole of His-438 is being formed to the imidazole N1 of His-438 and O2 of Glu-325, respectively. Therefore, the acylation step resembles a single-step double proton transfer mechanism, which is in accordance with the previous theoretical quantum mechanics (QM) calculations of Zhan et al. for the BChE catalyzed hydrolysis of cocaine (Zhan *et al.,* 2003). The intramolecular active bonds (carbonyl C=O (C1=O3), O1-H1 and N2-H2) are lengthened by 0.02, 0.20 and 0.49 Å, respectively, from the ES complex (Table 1). The O1H1N1 and N2H2O2 bond angles (177.2º and 179.5º, respectively) become more linear as compared to the ES complex. The $C_{carbonyl}$···O1 distance is shortened to 2.17 Å. As a result, the carbonyl carbon ($C_{carbonyl}$) is gradually distorted from the sp^2 structure to be more tetrahedral.

The hydrogen bonding between the carbonyl oxygen (O3) of cocaine and the oxyanion hole during the enzymatic reaction process is important for the transition state stabilization, espetially for the first acylation step. Each structure of ES, TS1 and INT1 have three NH-O3 hydrogen bond distances of 2.7-3.3 Å. The hydrogen bonds are shortened from ES to TS1 and to INT1   (Table 1). The increase of the hydrogen bond strength in the oxyanion hole can also be said to be a consequence of the increased electrostatic interaction. It can further be said that the catalytic activity of an enzyme seems to be an effect of the increased electrostatic stabilization of the hydrogen bonds in TS1 compared to ES.

The energy barrier from our work of 7.96 kcal/mol is larger than the corresponding values from Zhan et $al.,$ 2003, calculated at B3LYP/6-31+G(d) and B3LYP/6-31++G(d,p) levels of theory of 6.2 and 5.6 kcal/mol, respectively. The fact that the 6-31G+G(d) and 6-31G++(d,p) basis sets improve the accuracy for anions, compounds with lone pairs of electrons, and hydrogen-bonded dimmers which have significant electron density at large distances from the nuclei, was previously of concern due to the ionicity of the ES complex (Zhan et $al.,$ 2003). The energy barriers calculated by the addition of four highly diffuse functions (s, p_x, p_y, p_z) on each non-hydrogen atom and of a highly diffuse s function on each hydrogen atom were significantly lower than our results by 2.36 kcal/mol. Therefore, the single point energy calculations at B3LYP/6-31G++G(d,p) level of theory were tested. By using larger basis sets, we found that the energy barrier decreases to 5.92 kcal/mol, comparable with the previous values (Zhan et $al.,$ 2003).

After the double proton transfer process, the Ser-198 O1 is covalently attached to the carbonyl carbon (C1) of the benzyl ester, leading to the elongation of the carbonyl C1-O3 and C1-O4 bonds. The optimized geometry of the first intermediate (INT1) complex is depicted in Figure 10a. The C1-O3 bond distance (1.30 Å) is found to lie between the C-O double bond and the single bond of the ES complex (1.23 and 1.37 Å,

respectively). With respect to the ES and transition state complexes, the significant increment of the C1-O4 bond distance of the INT1 complex is responsible for the bond cleavage for the further step in the catalytic process.

The enzymatic oxyanion hole was frequently modeled either with ammonia or water molecules (Hu *et al.,* 1998). Here, we also describe the oxyanion hole with three amino acids, two glycines and one alanine (Figures 8b, 9b and 10b). Although, this model cannot properly represent the peptide chain, it reflects some steric hindrances of the enzyme framework that prevents the substrate's proximity to it. The distances between O3 and N atoms of the three amino acids are slightly increased in both ES and TS1 (Table1 and Figures 8b and 9b). Furthermore, we found that the use of three amino acids slightly reduces the energy barrier of the acylation process to 5.23 kcal/mol after being corrected by enlarging the basis sets. This may be due to the inclusion of some short-range effect of electrostatic potential from the oxyanion hole. Nevertheless, it does not perturb the geometrical structure of the catalytic significantly (Table1 and Figures 8b, 9b and 10b) since some dangling bonds of the catalytic triad are fixed while all are fully relaxed in the ammonia-oxyanion hole model. Considerable discrepancy of the structure can be seen in the INT1 (Table1 and Figure 10b).

The inclusion of electrostatic effects from the enzymatic framework was examined to demonstrate how the energy barrier of the reaction process could naturally be lowered. The optimized quantum mechanical clusters were embedded in the electrostatic field of the whole enzymatic framework and the single point energy calculations were then carried out. It can be seen that the energy barrier (5.07 kcal/mol) was significantly lowered by 2.89 kcal/mol from the small quantum cluster (7.96 kcal/mol) where the oxyanion hole was represented by three ammonia molecules. The single point energy correction at the 6-31++G(d,p) came out with the rather small energy barrier of 3.75 kcal/mol. This is, however, considered as an extreme electrostatic interaction case since the shielding effects from each layer of charges are ignored.

For systems with strong hydrogen bonding between solute and solvent molecules, the contributions of short-range nonelectrostaic interactions to the reaction energy surface maybe important. We examined the effect of nonspecific solute-solvent interaction using SCRF continuum solvation models. To mimic the acylation step of cocaine in an aqueous solution, the optimized quantum clusters were embedded in the polarized continuum model of water. The solute cavity surface is defined as overlapped spheres centered at the solute nuclei. Because the reaction produces a transition state that possesses zwitterionic characteristics, it can be expected to be significantly stabilized by polar solvents. Our results suggest that solvents help to speed up the reaction process (Table 2). The energy barrier of the acylation step is reduced to 6.71 kcal/mol in aqueous solution. Also, the INT1 is stabilized by 3.71 kcal/mol as compared to the gas phase model. The predicted energy barrier at 6-31G++(d,p) basis set is 4.51 kcal/mol, slightly higher than that of the electronic embedding model.

Scheme 1.   Schematic representation of the double-proton-transfer
mechanism for BChE-catalyzed hydrolysis of (-)-cocaine at the
benzoyl ester

ES

TS

INT
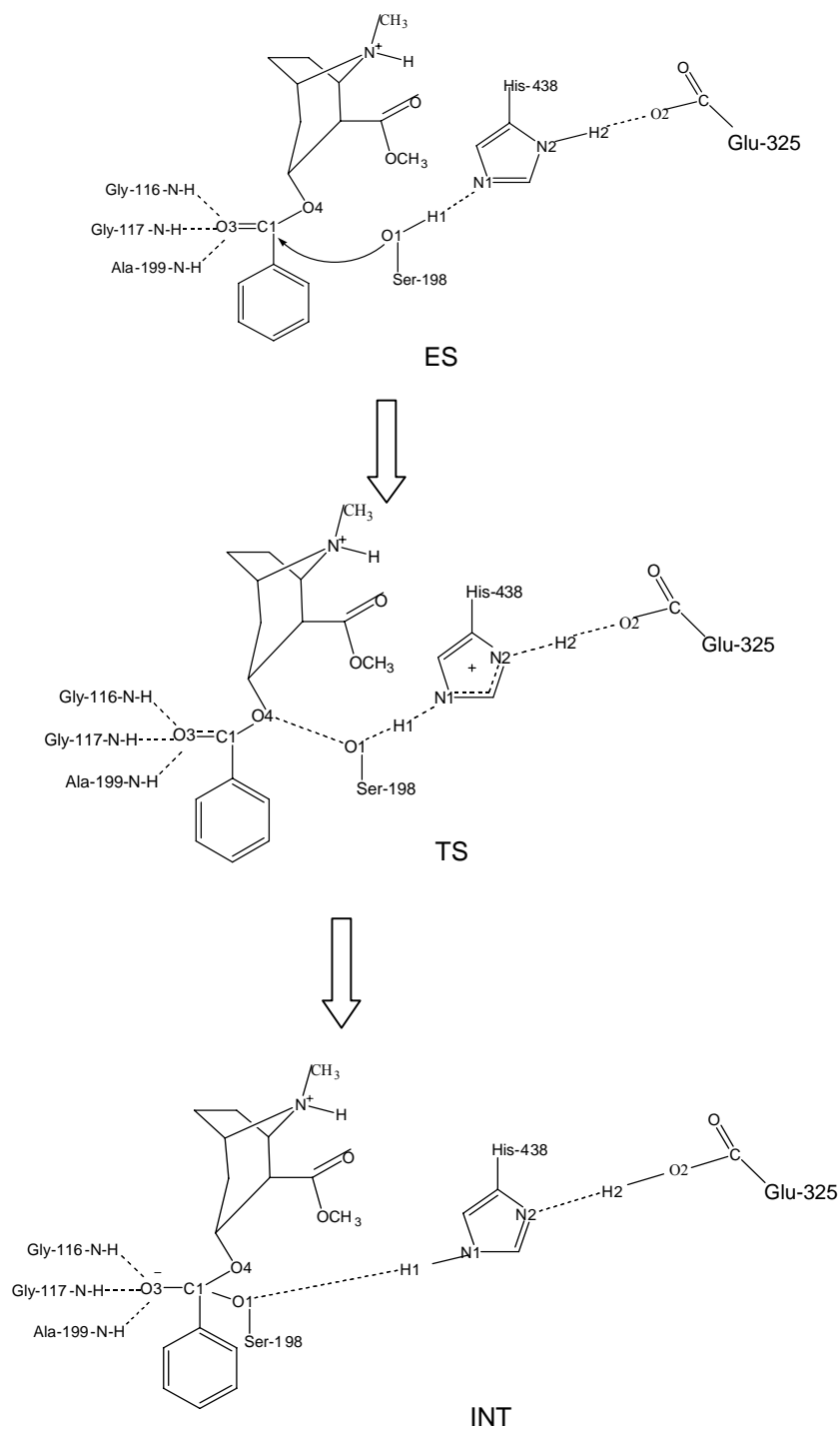
The basic BChE mechansim for the cocaine is like the the mechanism for ester hydrolysis in serine hydrolase and acetylcholinesterase (AChE). A possible reaction pathway for BChE-catalyzed hydrolysis of cocaine is shown in Scheme1 that illustrates cocaine and active groups of catalytic triad (Ser-198, His-438 and Glu-325) and the oxyanion hole (Gly-116, Gly-117 and Ala-199). The mechanism of the hydrolysis of cocaine in the acylation and deacylation steps is proposed in ester hydrolysis by Hu *et al.,* (1998). An important difference is the number of H-bonds formed between the carbonyl oxygen in the oxyanion hole and the peptidic NH groups in the three-pronged oxyanion hole. The three-pronged oxyanion hole in BChE is Gly-116, Gly-117 and Ala-199 is different from the two-pronged oxyanion hole in serine hydrolase.

Schematic representation of the reaction pathway for BChE hydrolysis of cocaine is depicted in Scheme 1, the acylation is initialized by the Ser-198 O1 attack at the carbonyl carbon of the cocaine benzoyl ester to form the first tetrahedral intermediate (INT1) through the first transition state (TS1). During the formation of INT1, the C-O bond between the carbonyl carbon and Ser-198 O1 gradually forms, while the proton at Ser-198 O1 gradually transfers to the imidazole N1 atom of His-438, which acts as a general base. This step prepared the bond cleavage for the deacylation step in the reaction pathway. At the same time the proton transfers between His-438 and Glu-325.

During the first step of acylation, the carbonyl oxygen strongly forms to three hydrogen bonds with the NH groups of Gly-116, Gly-117, and Ala-199. these potential hydrogen bonds are expected to increase in strength from ES to TS1 and to INT1 due to the expected increase of the net negative charge on the carbonyl oxygen.

Table 1 Optimized structural parameters of the catalytic triad and oxyanion hole for the Cluster and Cluster-amino models involved in the acylation step. Distances are in angstroms (Å) and angles in degrees.

Parameters	ES		TS1		INT1	
	Cluster	**Amino**	**Cluster**	**Amino**	**Cluster**	**Amino**
O1-H1	1.02	1.02	1.22	1.23	3.44	3.25
O1-N1	2.63	2.64	2.49	2.50	3.74	3.75
H1-N1	1.61	1.62	1.27	1.26	1.12	1.08
N2-H2	1.09	1.11	1.58	1.58	1.59	1.61
N2-O2	2.55	2.60	2.62	2.63	2.63	2.64
H2-O2	1.48	1.49	1.04	1.04	1.04	1.03
C1-O1	2.57	2.74	2.17	2.16	1.33	1.34
C1-O3	1.23	1.23	1.25	1.24	1.30	1.31
C1-O4	1.35	1.37	1.37	1.39	3.40	2.50
O4-H1	-	-	-	-	1.43	1.51
O3-N$_{(Gly-116)}$	3.04	3.12	2.97	3.09	2.94	2.76
N-H$_{(Gly-116)}$	1.01	1.02	1.02	1.02	1.02	1.02
O3-N$_{(Gly-117)}$	3.29	3.31	3.15	3.36	2.99	2.76
N-H$_{(Gly-117)}$	1.01	1.02	1.03	1.02	1.02	1.02
O3-N$_{(Ala-199)}$	3.11	3.40	3.19	3.33	2.97	2.86
N-H$_{(Ala-199)}$	1.00	1.02	1.02	1.02	1.02	1.02
∠O1-H1-N1	174.75	175.02	177.23	177.73	96.90	109.53
∠N2-H2-O2	173.70	179.15	179.51	179.11	178.50	178.05
Charge on O3	-0.559	-0.542	-0.567	-0.562	-0.577	-0.572

(8a)

(8b)
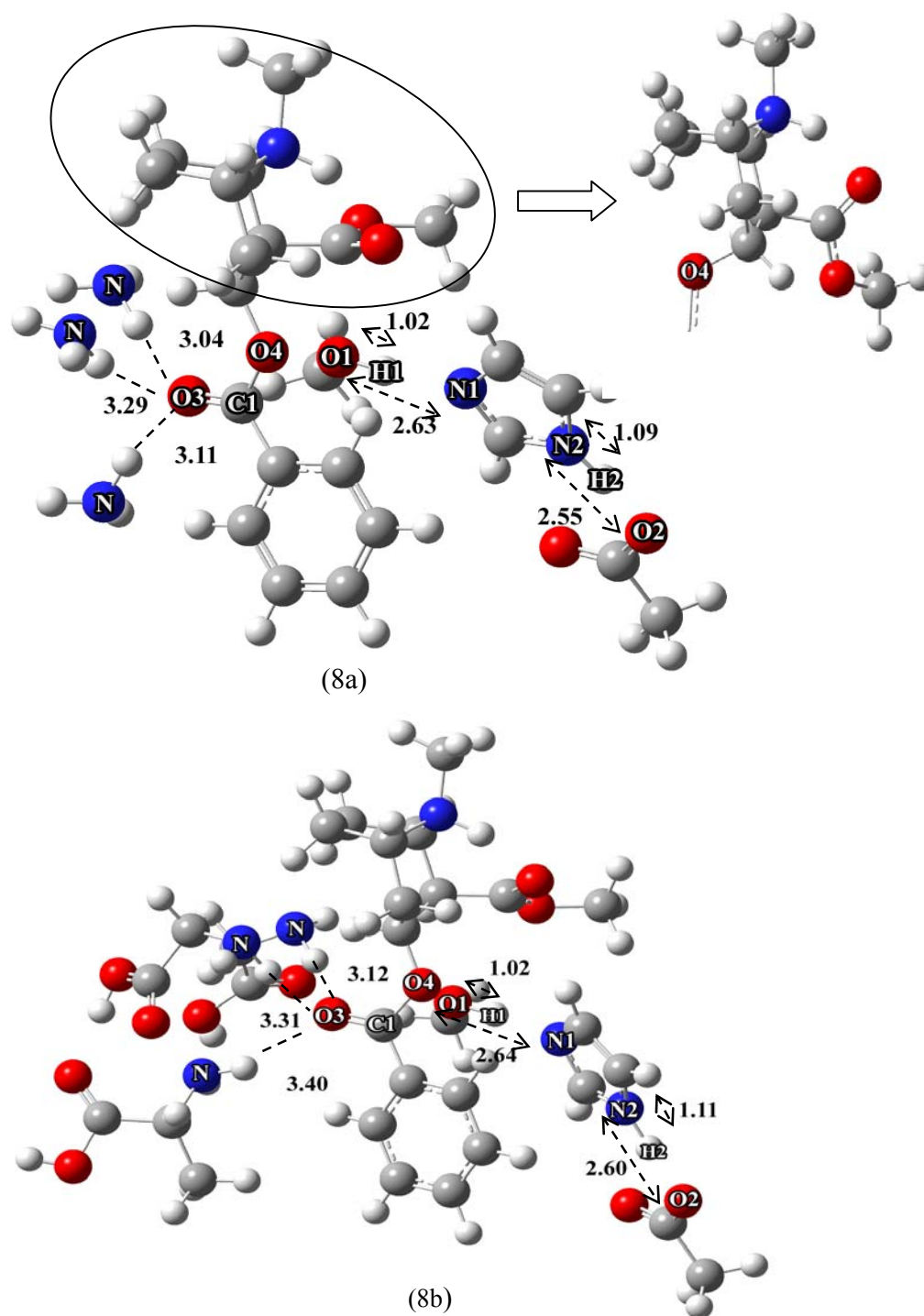
Figures 8   Representation of the ES-complex of butyrylcholinesterase:
(a) Cluster model; (b) Cluster amino model.
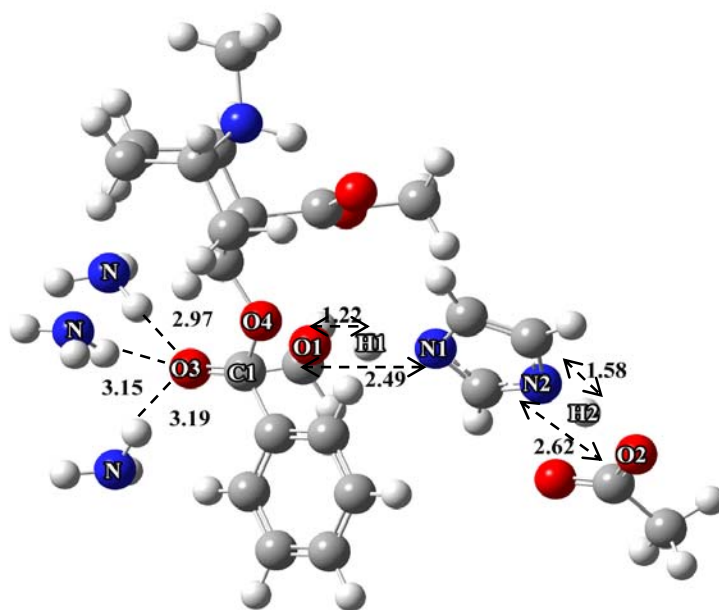
(9a)
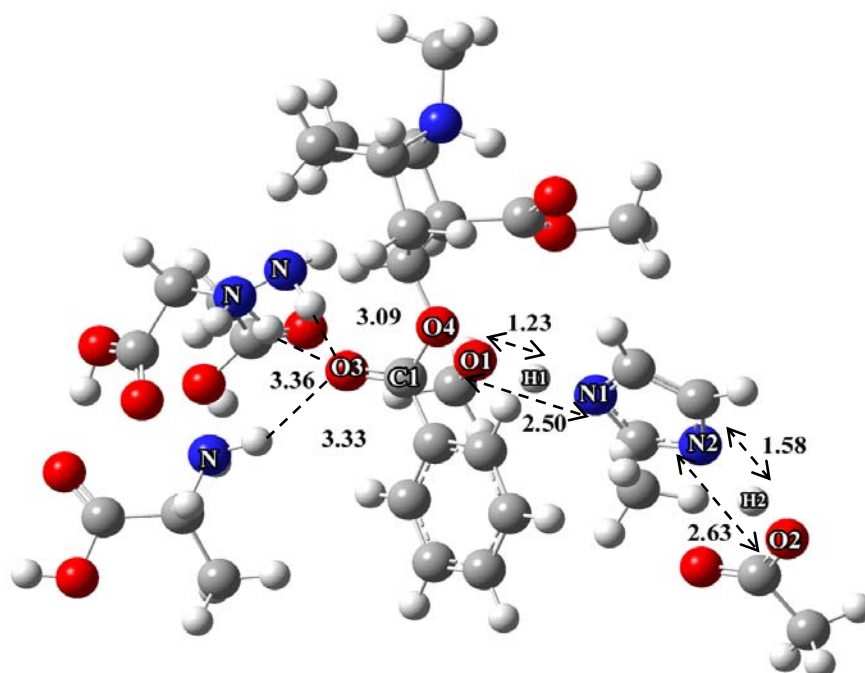
(9b)

Figures 9   Representation of the TS-complex of butyrylcholinesterase:

(a) Cluster model; (b) Cluster amino model.

(10a)

(10b)
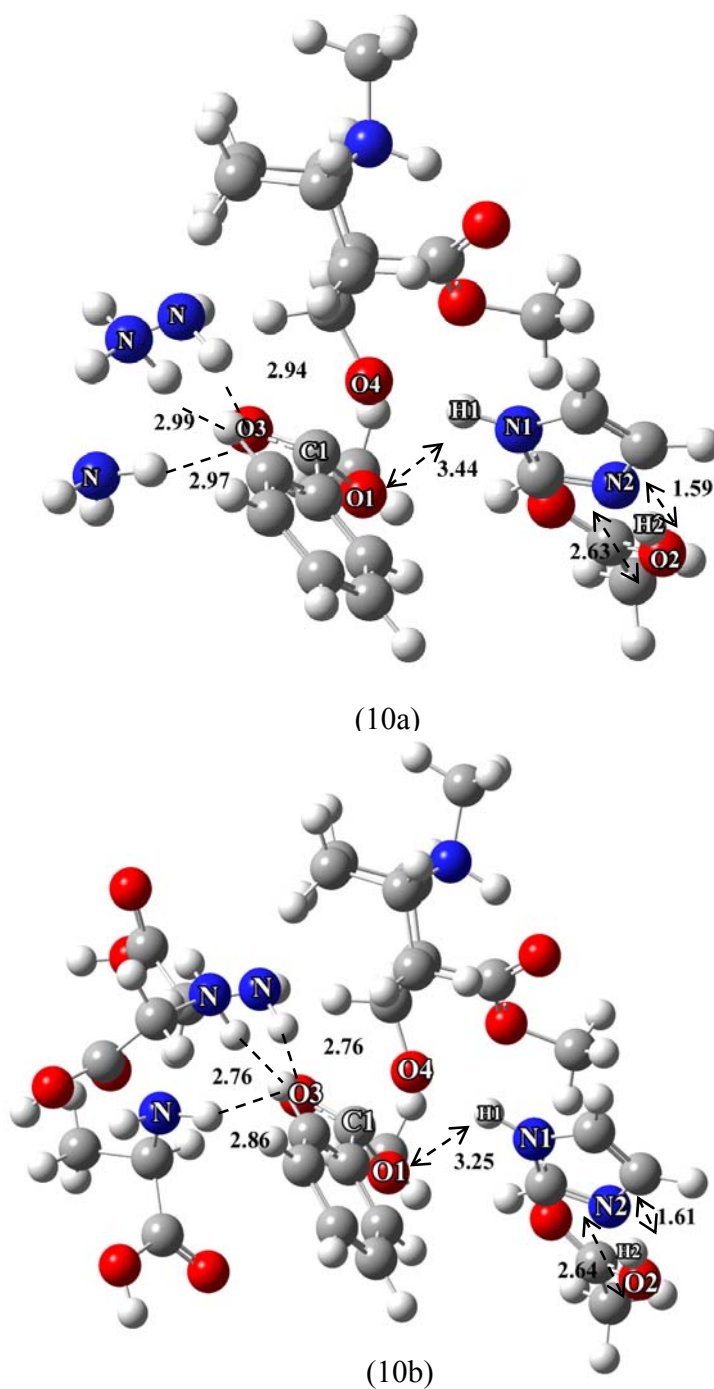
Figures 10   Representation of the INT-complex of butyrylcholinesterase:
(a) Cluster model; (b) Cluster amino model.

Table 2 Energy barriers of ES, TS1 and INT1-complex involved in the
acylation step (kcal/mol)

Models and Methods	TS1	INT1
B3LYP/6-31G(d,p)		
Cluster model	7.96	-14.62
Cluster amino model	7.63	-16.86
PCM model	6.71	-20.57
Embedding model	5.07	-25.23
B3LYP/6-31++G(d,p)		
Cluster model	5.92	-18.28
Cluster amino model	5.23	-22.64
PCM model	4.51	-27.65
Embedding model	3.75	-30.29

CONCLUSION

The geometries and the energy barriers of the transition state, intermediate, and prereactive enzyme-substrate complex (ES) involved in the BChE-catalyzed hydrolysis of cocaine have been determined by performing the embedded calculations on the first step of acylation process. The PCM and embedded calculations allow us to account for short-range nonelectrostatic and long-range electrostatic interactions of the protein environment effects on the pathway and the energy barriers of these enzymatic reactions. The energy barriers of this step lie between the values obtained by using the PCM and embedded calculations because, in nature, both effects should be explicitly taken into considersation.

First, the cluster model and the cluster-amino model were optimized at the B3LYP/6-31G(d,p) level of theory. The energy barriers of the cluster-amino model, 7.63 kcal/mol, is lower than those of the cluster model, 0.33 kcal/mol. This comes from the inclusion of some short-range effects of the electrostatic potential from the oxyanion hole. However, optimized geometry parameters do not change significantly from the cluster model.

The prediction of energy barriers by single point energy calculations at B3LYP/6-31++G(d,p) of PCM and the embedded model is 4.51 and 3.75 kcal/mol, respectively, approximately less than that of the cluster model by 20-40%. These stabilized energies suggest that the effect of short-range and long-range interactions is effective with the substrate molecule on the active region in addition to the effect of the enzyme framework.

The results obtained in this present study suggest that the PCM and Embedded calculations provide an efficient and accurate way for studying the energy barriers of BChE-catalyzed hydrolysis of cocaine.

LITERATURE CITED

Aldridge, W. N. 1953. Serum esterases. 2. An enzyme hydrolysing diethyl p-nitrophenyl phosphate (E 600) and its identity with the A-esterase of mammalian sera. **Biochem J.** 53: 117-124.

Allon, N., L. Raveh, E. Gilat, E. Cohen, J. Grunwald and Y. Ashani. 1998. Prophylaxis against soman inhalation toxicity in guinea pigs by pretreatment alone with human Serum butyrylcholinesterase. **Toxicol. Sci.** 43: 121-128.

Bachovchin, W. W. and J. D. Roberts. 1978. Nitrogen-15 nuclear magnetic resonance spectroscopy. The state of histidine in the catalytic triad of alpha.-lytic protease. Implications for the charge-relay mechanism of peptide-bond cleavage by serine proteases. **J. Am. Chem. Soc.** 100: 8041-8047.

Barak, D, C. Kronman, A. Ordentlich, N. Ariel, A. Bromberg, D. Marcus, A. Lazar, B. Velan, A. Shafferman. 1994. Acetylcholinesterase peripheral anionic site degeneracy conferred by amino acid arrays sharing a common core. **J. Biol. Chem.** 269: 6296-6305.

Behra, M., X. Cousin, C. Bertrand, J. L. Vonesch, D. Biellmann, A. Chatonnet and U. Strahle. 2002. Acetylcholinesterase is required for neuronal and muscular development in the zebrafish embryo. **Nat. Neurosci.** 5: 111-118.

Berkman, C. E., G. E. Underiner and J. R. Cashman. 1997. Stereoselective inhibition of human butyrylcholinesterase by phosphonothiolate analogs of (+)- and (-)-coaine. **Biochem. Pharmcol.** 54: 1261.

Blow, D. M., J. J. Birktoft and B. S. Hartley. 1969. Role of a buried acid group in the mechanism of action of chymotrpsin. **Nature** 221: 337-340.

Bourne, Y, P. Taylor, Z. Radic, and P. Marchot. 2003. Structural insights into ligand interactions at the acetylcholinesterase peripheral anionic site. **EMBO J.** 22: 1-12.

Broomfield, C. A., D. M. Maxwell, R. P. Solana, C. A. Castro, A. V. Finger and D. E. Lenz. 1991. Protection by butyrylcholinesterase against organophosphorus poisoning in nonhuman primates. **J. Pharmacol. Exp. Ther.** 259: 633-638.

Bui, J. M., R. H. Henchman, and J. A. McCammon. 2003. The Dynamics of Ligand Barrier Crossing inside the Acetylcholinesterase Gorge. **Biophys. J.** 85: 2267-2272.

Carrera, M. R., J. A. Ashley, P. Wirsching, G. F. Koob and K.D. Janda. 2000. Cocaine vaccines: antibody protection against relapse in a rat model. **Proc. Natl. Acad. Sci. U.S.A.** 97: 6202-6206.

_____, _____, _____, _____, _____. 2001. A second-generation vaccine protects against the psychoactive effects of cocaine. **Proc. Natl. Acad. Sci. U.S.A.** 98: 1988-1992.

_____, _____, _____, _____, _____, and L. H. Parsons 1995. Suppression of psychoactive effects of cocaine by active immunization. **Nature** 378: 727-730.

Carroll, F. I., L. L. Howell and M. J. Kuhar. 1999. Pharmacotherapies for Treatment   of Cocaine Abuse: Preclinical Aspects. **J. Med. Chem.** 42: 2721-2736.

Chipman, D. 1997. Charge penetration in dielectric models of solvation. **J. Chem. Phys.** 106: 10194-10206.

_____. 1999. Simulation of volume polarization in reaction field theory. **J. Chem. Phys.** 110: 8012-8018.

_____. 2000. Reaction field treatment of charge penetration. **J. Chem. Phys.** 112: 5558-5565.

Cleland, W. W. and M. M. Kreevoy. 1994. Low-barrier hydrogen bonds and enzymic catalysis**. Science** 264: 1887-1890.

Cossi, M., V. Barone, R. Cammi, J. Tomasi. 1996. Ab initio study of solvated molecules: a new implementation of the polarization continuum model. **Chem. Phys. Lett.** 255: 327-335.

Cramer, C. J and D. G. Truhar. 1999. Implicit solvation models: equilibria, structure, spectra, and dynamics. **Chem. Rev.** 99: 2161-2200.

Daggett, v., S. Schroeder, P. Kollman. 1991. Catalytic pathway of serine proteases: classical and quantum mechanical calculations**. J. Am. Chem. Soc.** 113:   8926-8935.

Dapprich, S., I. Komaromi, K.S. Byun, K. Morokuma and M.J. Frisch. 1999. A new ONIOM implementation in Gaussian98. Part I. The calculation of energies, gradients, vibrational frequencies and electric field derivatives. **J. Mol. Struct.**

(Theochem) 461: 1-21.

De Ferrari, G. V., W. D. Mallender, N. C. Inestrosa and T. L. Rosenberry. 2001. Thioflavin T Is a Fluorescent Probe of the Acetylcholinesterase Peripheral Site That Reveals Conformational Interactions between the Peripheral and Acylation Sites**. J. Biol. Chem.** 276: 23282-23287.

De Prada, P., G. Winger and D. W. Landry. 2000. Application of artificial enzymes to the problem of cocaine. **Ann. N. Y. Acad. Sci.** 909: 159-169.

Dungsrikaew, V., J. Limtrakul, K. Hermansson and M. Probst. 2004. Comparison of methods for point-charge representation of electrostatic fields. **Int. J. Quantum Chem.** 96: 17-22.

Ekholm, M. and H. Konschin. 1999. Comparative model building of human butyrylcholinesterase. **J. Mol. Struct. (THEOCHEM)** 467: 161-172.

Ettinger, R. H., W. F. Ettinger and W. E. Harless. 1997. Active immunization with cocaine-protein conjugate attenuates cocaine effects. **Pharmacol. Biochem. Behav.** 58: 215-220.

Fairclough, R. A. and C. N. Hinshelwood. 1937. The functional relationship between the constants of the Arrhenius equation. Solvent effects in the formation of quaternary ammonium salts. **J. Chem. Soc.** 538.

Feig, M. and C. L. Brooks III. 2004. Recent advances in the development and application of implicit solvent models in biomolecule simulations. **Curr. Op. Struct. Biol.** 14:217–224.

Felder, C. E., S. A. Botti, S. Lifson, I. Silman, and J. L. Sussman. 1997. External and internal electrostatic potentials of cholinesterase models. **J. Mol. Graphics Modelling** 15: 318-327.

Fox, B. 1997. Development of a therapeutic vaccine for the treatment of cocaine addiction. **Drug Alcohol Depend.** 100: 153.

Fox, B. S., K. M. Kantak, M. A. Edwards, K. M. Black, B. K. Bollinger, A. J. Botka, T. L. French, T. L. Thompson, V. C. Schad, J. L. Greenstein, M. L. Gefter, M. A. Exley, P. A. Swain and T. J. Briner. 1996. Efficacy of a therapeutic cocaine vaccine in rodent models. *Nat. Med.* 2: 1129-1132.

Frey, P. A. 1995. **Science** 269 :104-106.

_____, S. A. Whitt, and J. B. Tobin. 1994. A low-barrier hydrogen bond in the catalytic triad of serine proteases**. Science** 264: 1927-1930.

Frisch, M.J., G.W. Trucks, H.B. Schllegel, G.E. Scuseria, M.A. Robb, J.R. Cheeseman, V.G. Zakrzewski, J.A. Montgomery, R.E. Stratmann, J.C. Burant, S. Dapprich, J.M. Millam, A.D. Daniels, K.N. Kudin, M.C. Strain, O. Farkas, J. Tomasi, V. Barone, M. Cossi, R. Cammi, B. Mennucci, C. Pomelli, C. Adamo, S. Clifford, J. Ochterski, G.A. Petersson, P.Y. Ayala, Q. Cui, K. Morokuma, D.K. Malick, A. Rabuck, K. Raghavachari, J.B. Foresman, J. Cioslowski, J.V. Ortiz, B. Stefanov, G. Liu, A. Liashenko, P. Piskorz, I. Komaromi, R. Gomperts, R.L. Martin, D.J. Fox, T. Keith, M.A. Al-Laham, C.Y. Peng, A. Nanayakkara, C. Gonzalez, M. Challacombe, P.M.W. Gill, B.G. Johnson, W. Chen, M.W. Wong, J.L. Andres, M. Head-Gordon, E.S. Replogle and J.A. Pople. 1998. **Gaussian 98 (Revision A.7)**. Pittsburgh, PA.

Fuxreiter, M. and A. Warshel. 1998. Origin of the catalytic power of acetylcholinesterase: computer simulation studies**. J. Am. Chem. Soc.** 120: 183-194.

Gerlt, J. A. and P. G. Gassman. 1993. An explanation for rapid enzyme-catalyzed proton abstraction from carbon acids : importance of late transition states in concerted mechanisms. **J. Am. Chem. Soc.** 115: 11552.

Golubev, N. S., V. A. Gindin, and S. S. Ligai. 1994. **Biochemistry (Moscow)** 59: 447.

Gorelick, D. A. 1997. Enhancing cocaine metabolism with butyrylcholinesterasse   as a treatment strategy. **Drug Alcohol Depend.** 48: 159.

Greatbanks, S.P., I.H. Hillier, N.A. Burton and P. Sherwood. 1996. Adsorption   of water and methanol on zeolite Brønsted acid sites: An ab initio,   embedded cluster study including electron correlation. **J. Chem. Phys.** 105: 3770-3776.

Harel, M., G. Kryger, T. L. Rosenberry, W. D. Mallender, T. Lewis, R. J. Fletcher, J. M. Guss, I. Silman, and J. Sussman. 2000. Three-dimensional structures of *Drosophila melanogaster* acetylcholinesterase and of its complexes with two potent inhibitors. **Protein Sci.** 9: 1063-1072.

_____, I. Schalk, L. Ehret-Sabatier, F. Bouet, M. Goeldner, C. Hirth, P. H. Axelsen, I. Silman and J. L. Sussman. 1993. Quaternary ligand binding to aromatic residues in the active-site gorge of acetylcholinesterase. **Proc. Natl. Acad. Sci. U. S. A.** 90: 9031-9035.

_____, J. L. Sussman, E. Krejci, S. Bon, P. Chanal, J. Massoulie and I. Silman. 1992. Conversion of acetycholinesterase to butyrylcholinesterase modeling and mutagenesis. **Proc. Natl. Acad. Sci. U. S. A.** 89: 10827.

Hillier, H.I. 1999. Chemical reactivity studied by hybrid QM/MM methods. **THEOCHEM** 463 (1-2): 45-52.

Hu, C.-H., T. Brick and K. Hult. 1998. Ab initio and density functional theory studies of the catalytic mechanism for ester hydrolysis in serine hydrolases. **Int. J. Quantum Chem.** 69: 89-103.

Hurley, M. M., J.B. Wright, G.H. Lushington, W.E. White. 1997. Quantum mechanics and mixed quantum mechanics/molecular mechanics simulations of model nerve agents with acetylcholinesterase. Theoretica Chimica Acta. 109: 160-168.

Hwang, J. K. and A. Warshel. 1987. Semiquantitative calculations of catalytic free energies in genetically modified enzymes. **Biochemistry** 26: 2669-2673.

Injan , N., N. Pannorad, M. Probst, and J. Limtrakul. 2005. Pyridine adsorbed on H-Faujasite zeolite: Electrostatic effect of the infinite crystal lattice calculated from a point charge representation. **Int. J. Quantum Chem.** 105: 898-905.

Jandsang, B., T. Nanok and J. Limtrakul. 2006. Structures and Reaction Mechanisms of Cumene Formation via Benzene Alkylation with Propylene in a Newly Synthesized ITQ-24 Zeolite: An Embedded ONIOM Study. **J. Phys. Chem. B.** 110: 12626-12631.

Kantak, K. M., S. L. Collins, E. G. Lipman, J. Bond, K. Giovanoni and B. S. Fox. 2000. Evaluation of anti-cocaine antibodies and a cocaine vaccine in a rat self-administration model. **Psychopharmacology** 148: 251-262.

Ketrat, S. and J. Limtrakul. 2003. Theoretical study of the adsorption of ethylene on alkali-exchanged zeolites. **Int. J. Quantum. Chem.** 94: 333-340.

Knapp, E. W., P. Vagedes, J. Marelius, J. Aaqvist, and B. Rabenstein. 2000. The deacylation step of acetylcholinesterase: computer simulation stuides. **J. Am. Chem. Soc.** 122: 12254-12262

Koca, J., C.-G. Zhan, R. C. Rittenhouse, and R. L. Ornstein. 2001. Mobility of the Active Site Bound Paraoxon and Sarin in Zinc-Phosphotriesterase by Molecular Dynamics Simulation and Quantum Chemical Calculation. **J. Am. Chem. Soc.** 123: 817 -826.

Landry, D. W. and G. X.-Q. Yang. 1997. Anti-cocaine catalytic antibodies − a novel aproach to the problem of addiction. **J. Addict. Dis.** 16: 1.

Levy, R. M. and E. Gallicchio. 1998. Computer simulations with explicit solvent: recent progress in the thermodynamic decomposition of free energies and in modeling electrostatic effects. **Ann. Rev. Phys. Chem.** 49:531–567.

Lomratsiri, J., M. Probst and J. Limtrakul. 2006. Structure and adsorption of a basic probe molecule on H-ZSM-5 nanostructured zeolite: An embedded ONIOM study. **J. Mol. Graphics Modelling** 25: 219-225.

Limtrakul, J. 1995. Adsorption of methanol in zeolite, gallosilicate and SAPO catalysts. **Chem. Phys.** 193: 79-87.

_____, P. Khongpracha, S. Jungsuttiwong and T.N. Truong. 2000b. Adsorption of carbon monoxide in H-ZSM-5 and Li-ZSM-5 zeolites: an embedded ab initio cluster study. **J. Mol. Cat. A** 153: 155-163.

_____, P. Chuichay and S. Nokbin. 2001a. Effect of high coverages on proton transfer in the zeolite/water system. **J. Mol. Struct.** 560: 169-177.

_____, S. Jungsuttiwong and P. Khongpracha. 2000a. Adsorption of carbon monoxide on H-FAU and Li-FAU zeolites: an embedded cluster approach. **J. Mol. Struct.** 525: 153-162.

_____, T. Nanok, P. Khongpracha, S. Jungsuttiwong and T.N. Truong. 2001b. Adsorption of unsaturated hydrocarbons on zeolites: the effects of the zeolite framework on adsorption properties of ethylene. **Chem. Phys. Lett.** 349: 161-166.

Lockridge, O., C. F. Bartels, T. A. Vaughan, C. K. Wong, S. E. Norton and L. L. Johnson. 1987 **J. Biol. Chem.** 262: 549.

_____ and P. Masson 2000. Pesticides and susceptible populations: people with butyrylcholinesterase genetic variants may be at risk. **Neurotoxicology.** 21: 113-126.

_____ , R. M. Blong, P. Masson, M.-T. Fronment, C. B. Millard andC.A. Broomfield. 1997. A single amino acid substitution, Gly117His, confers phosphotriesterase (organophosphorus acid anhydride hydrolase) activity on human butyrylcholinesterase. **Biochemistry** 36: 786-795.

_____, S. Adkins and B. N. La Du. 1987 **J. Biol. Chem.** 262: 12945.

MacPhee-Quigley, K., T. S. Vedvick, P. Taylor and S. S. Taylor. 1986 **J. Biol. Chem.** 261:13565.

Mack, A. and A. Robitzki. 2000. The key role of butyrylcholinesterase during neurogenesis and neural disorders: an antisense-5'butyrylcholinesterase-DNA study. **Prog Neurobiol.** 60: 607-628.

Massiah, M. A., C. Virage, P. M. Reddy, I. M. Kovach, J. Johnson, T. L.   Rosenberry and A. S. Mildvan. 2001. Short, strong hydrogen bonds at   the   active   site   of human acetylcholinesterase: proton NMR studies**.   Biocheimistry**   40:5682-5690.

Masson, P., C. Clery, P. Guerra, A. Redslob, C. Albaret, and P.-L. Fortier. 1999. Hydration   change   during   the   aging   of   phosphorylated   human butyrylcholinesterase: Importance of residues aspatate-70 and Glutamate-197 in the water network as probed by hydrostatic osmotic pressure. **Biochem. J.** 343: 361-369.

_____, C. M.-T. Froment, C. F. Bartels, and O. Lockridge. 1996. Asp70   in the peripherical anionic site of human butyrylcholinesterase. **Eur. J. Biochem.** 235: 36-48.

_____, F. Nachon, C. F. Bartels, M.-T. Froment, F. Ribes, C. Matthews, and O. Lockridge. 2003. High activity of human butyrylcholinesterase at low pH in the presence of excess butyrylcholinesterase. **Eur. J. Biochem.** 270: 315-324.

_____, P. Legrand, C. F. Bartels, M.-T. Froment, L. M. Schopfer and O. Lockridge. 1997. Role of aspartate 70 and tryptophan 82 in binding of succinyldithiocholine to human butyrylcholinesterase. **Biochemistry** 36: 2266-2277.

_____, W. Xie, M.-T. Froment, V. Levitsky, P.-L. Fortier, C. Albaret, O. Lockridge 1999. Interaction between the periph-eral site residues of human butyrylcholinesterase, D70 and Y332, in binding and hydrolysis of substrates. **Biochim. Biophys. Acta** 1433: 281-293.

_____, W. Xie, M.-T. Froment, O. Lockridge. 2001. Effects of mutations of active site residues and amino acids interacting with Ω loop on substrate activation of butyrylcholinesterase. **Biochim. Biophys. Acta** 1544: 166-176.

Massoulie, J., J. Sussman, S. Bon, and I. Silman. 1993. Structure and functions of acetylcholinesterase and butyrylcholinesterase. **Prog. Brain Res.** 98: 139-146.

_____. and S. Bon. 1982. The molecular forms of cholinesterase and acetylcholinesterase in vertebrates. **Annu. Rev. Neurosci.** 5: 57-106.

Meshorer, E., C. Erb, R. Gazit, L. Pavlovsky, D. Kaufer, A. Friedman, D. Glick. N. Ben-Arie, and H. Soreq. 2002. Alternative Splicing and Neuritic mRNA Translocation Under Long-Term Neuronal Hypersensitivity. **Science** 295: 508-512.

Miertus, S., E. Scrocco, J. Tomasi. 1981. Electrostatic interaction of a solute with a continuum. A direct utilizaion of AB initio molecular potentials for the prevision of solvent effects. **Chem. Phys.** 55 :117-129.

_____ and J. Tomasi. 1982. Approximate evaluations of the electrostatic free energy and internal energy changes in solution processes. **Chem. Phys.** 65: 239-245.

Millard, C. B., O. Lockridge and C. A. Broomfield. 1995. Design and expression of organophosphorus acid anhydride hydrolase activity in human butyrylcholinesterase**. Biochemistry** 34: 15925-15933.

_____ , _____ and _____ . 1998. Organophosphorus acid anhydride hydrolase activity in human butyrylcholinesterase: synergy results in a somanase. **Biochemistry** 37: 237-247.

Nachon, F., L. Ehret-Sabatier, D. Loew, C. Colas, A. van Dorsselaer, and M. Goeldner. 1998. Trp82 and Tyr332 Are Involved in Two Quaternary Ammonium Binding Domains of Human Butyrylcholinesterase as Revealed by Photoaffinity Labeling with [^{3}H]DDF**. Biochemistry** 37: 10507-10513.

Nicolet, Y., O. Lockridge, P. Masson, J. C. Fontecilla-Camps, and F. Nachon. 2003. Crystal structure of human butyrylcholinesterase and of its complexes with substrate and products. **J. Biol. Chem.** 278: 41141-41147.

Ott, P. 1985. Membrane acetylcholinesterases: purification, molecular properties and interactions with amphiphilic environments. **Biochim. Biophys. Acta.** 822: 375-392.

Quinn, D. 1987. Acetylcholinesterase: enzyme structure, reaction dynamics, and virtual transition states. **Chem. Rev.** 87: 955-979.

Rabenstein, B. 2000. Monte Carlo methods for simulation of protein folding and titration. **PhD thesis, Freie Universität Berlin**.

_____, G. M. Ullmann, and E.W. Knapp. 1998. Calculation of protonation patterns in proteins with structural relaxations and molecular ensembles - application to the photosynthetic reaction center. **Eur. Biophys. J.** 27:626–637.

Richter, R. M.; E. M Pich, G. F. Koob, and F. Weiss. 1995. Sensitization of cocaine-stimulated increase in extracellular levels of corticotropin- releasing from the rat amygdala after repeated administration as determined by intracranial microdialysis. **Neurosci. Lett.** 187: 169-172

_____, and F. Weiss. 1999. In vivo CRF release in rat amygdala is increased during withdrawal after cocaine self-administration with unlimited access. **J. Neurosci**. 34: 254-261.

Rodriguez, D. F., F., M.R.A. Carrera, M. Navarro, G.F. Koob, and F. Weiss. 1997. Activation of corticotropin releasing factor in the limbic system during cannabinoid withdrawal. **Science** 276: 2050-2054.

Rotundo, R. L. 1984. Asymmetric acetylcholinesterase is assembled in the golgi apparatus. **Proc. Natl. Acad. Aci. U. S. A.** 81: 479-483.

Rylander, P. N. and D. S. Tarbell. 1950. Cleavage of the carbon-sulfur bond. Rates of hydrolysis of some alkyl acetates and the corresponding thiolacetates   in aqueous acetone. **J. Am. Chem. Soc.** 72: 3021-3025.

Saxena, A., A. M. G. Redman, X. Jiang, O. Lockridge and B. P. Doctor. 1997. Differences in active site gorge dimensions of cholinesterases revealed by binding of inhibitors   to human butyrylcholinesterase. **Biochemistry** 36:

14642- 14651.

Scheiner, S., K. Tapas. 1995. The nonexistence of specially stabilized hydrogen bonds in enzymes. **J. Am. Chem. Soc.** 117: 6970-6975.

Schumacher, M., S. Camp, Y. Maulet, M. Newton, K. MacPhee-Quigley, S. S. Taylor, T. Friedman and P. Taylor. 1986 **Nature (London)** 319: 407.

Sholten, J. D., J. L. Hogg, and F. M. Raushel. 1988. Methyl chymotrypsin catalyzed hydrolyses of specific substrate esters indicate multiple proton catalysis is possible with a modified charge relay triad. **J. Am. Chem. Soc.** 110: 8246-8247.

Silman, I., and J. L. Sussman. 2005. Acetylcholinesterases: "Classical" and "non-classical" functions and pharmacology. **Curr. Opin. Pharmacol.** 5: 293-302.

_____, L. Giamberardino, J. M. Lyles, J. Y. Couraud, E. A. Barnard. 1979. Parallel regulation of acetylcholinesterase and pseudocholinesterase in normal, denervated and dystrophic chicken skelton muscle. **Nature (London)** 280: 160-162.

Sinclair, P.E., A.H. de Vries, P. Sherwood, C.R.A. Catlow and R.A. van Santen.1998. Quantum-chemical studies of alkene chemisorption in chabazite: A comparison of cluster and embedded-cluster models. **J. Chem. Soc. Faraday Trans.** 94: 3401-3408.

Singh, S. 2000. Chemistry, Design, and Structure-Activity Relationship of Cocaine Antagonists**. Chem. Rev.** 100: 925-1024.

Sparenborg, S., F. Vocci and S. Zukin. 1997. Peripheral cocaine-blocking agents: new medications for cocaine dependence. An introduction to immunological and enzymatic approaches to treating cocaine dependence reported by Fox, Gorelick and Cohen in the immediately succeeding articles. **Drug Alcohol Depend.** 48: 149.

Stefan, P., M. R. Tabet, C. D. Farr, A. B. Norman, and W. James Ball, Jr. 2004. Three-dimensional quantitative structure-activity relationship modeling of cocaine binding by a novel human monoclonal antibody. **J. Med. Chem.** 47: 133-142

Stojan, J., M. Golicnik, M.-T. Froment, F. Estour, and P. Masson. 2002. Concentration-dependent reverible activation-inhibition of human butyrylcholinesterase by tetraethylammonium ion. **Eur. J. Biochem.** 269.

Suarez, D. And M. J. Field. 2005. Molecular dynamics simulations of human butyrylcholinesterase. **Proteins: Struct., Funct., Bioinf.** 59: 104.117.

Sun, H., J. E. Yazal, O. Lockridge, L. M. Schopfer, S. Brimijoin and Y.-P. Pang. 2001. Predicted Michaelis-Menten complexes of cocaine- butyrylcholinesterase. **J. Biol. Chem.** 276: 9330-9336.

Sussman, J.L., M. Harel, F. Frolow, C. Oefner, A. Goldman, L. Toker and L. Silman. 1991. Atomic structure of acetylcholinesterase from *Torpedo californica*: a prototypic acetylcholine-binding protein. **Science** 253: 872-879.

Szegletes, T., W. D. Mallender, P. J. Thomas, and T. L. Rosenberry, 1999. Substrate Binding to the Peripheral Site of Acetylcholinesterase Initiates Enzymatic Catalysis. Substrate Inhibition Arises as a Secondary Effect. **Biochemistry** 38: 122-133.

Tai, K., T. Shen, U. Börjesson, M. Philippopoulos, and J. A. McCammon. 2001. Analysis of a 10-ns molecular dynamics simulation of mouse acetylcholinesterase. **Biophys. J.** 81: 715-724.

Tomasi, J. and M. Persico. 1994. Molecular interactions in solution: an overview of methods based on continuous distributions of the solvent. **Chem. Rev.** 94: 2027-2094.

Ullmann, G. M. and E. W. Knapp. 1999. Electrostatic models for computing protonation and redox equilibria in proteins. **Eur. Biophys. J.** 28:533–551.

Warshel, A., and A. Papazyan. 1996. Energy considerations show that low-barrier hydrogen bonds do not offer a catalytic advantage over ordinary hydrogen bonds. **Proc. Natl. Acad. Sci. USA.** 93:13665-13670.

_____, A. Papazyan, and P. A. Kollman. 1995. On low-barrier hydrogen bonds and enzyme catalysis. **Science** 269: 102-104.

_____, A. Papazyan, and I. Muegge. 1997. Microscopic and semimacroscopic redox calculations: what can and cannot be learned from continuum models. **J. Biol. Inorg. Chem.** 2:143–152, 1997.

_____, A., G. Naray-Szabo, F. Sussman and J. K. Hwang. 1989. How do serine proteases really work? **Biochemistry** 28(9); 3629-3637.

_____, _____, _____ and _____. 1989. How do serine proteases really work? **Biochemistry.** 28(9): 3629-3637.

_____. and   S. Ressell. 1986. Theoretical correlation of structure and energetics in   the catalytic reaction of trypsin. **J. Am. Chem. Soc.** 108:   6569-6579.

Weiss, F. L.H. Parsons, and A. Markou. 1995. Neurochemistry of cocaine withdrawal. In: **The Neurobiology of Cocaine: Cellular and   Molecular   Mechanisms. Hammer, Jr., R.L., ed. Boca Raton, FL:** 163-180.

Wlodek, S. T., J. Antosiewwicz, and J. M. Briggs. 1997. On the Mechanism of Acetylcholinesterase Action: The Electrostatically Induced Acceleration of the Catalytic Acylation Step. **J. Am. Chem. Soc.** 119: 8159-8165.

Xie, W., C. V. Altamirano, C. F. Bartels, R. J. Speirs, J. R. Cashman, O.   Lockridge, L. M. Schopfer, S. Brimijoin and Y.-P. Pang. 2001.   Predicted Michaelis-Menten complexes of cocaine-butyrylcholinesterase: engineering   effective butyrylcholinesterase mutants for cocaine   detoxication. **J. Biol. Chem.** 276: 9330.

Yang, G., J. Chun, H. Arakawan-Uramoto, X. Wang, M. A. Gawinowicz, K. Zhao and   D. W. Landry 1996. Anti-cocaine catalytic antibodies: a synthetic approach to improved antibody diversity. **J. Am. Chem. Soc.** 118: 5881.

Zhan, C.-G. and D. Gao. 2005. Catalytic mechanism and enrgy barriers for butyrylcholinesterase-catalyzed hydrolysis of cocaine. **Biophys. J.** 89: 3863-3872.

_____ and D. W. Landry. 2001. Theoretical studies of competing reaction pathways and energy barriers for alkaline ester hydrolysis of cocaine. **J. Phys. Chem.** 105: 1296-1301.

_____ , D. W. Landry, and R. L. Ornstein. 2000. Energy barriers for alkaline hydrolysis of carboxylic acid esters in aqueous solution by reaction field calculations. **J. Phys. Chem. A** 104: 7672-7678.

_____ , _____ , and _____ . 2000. Reaction pathways and energy barriers for alkaline hydrolysis of carboxylic acid esters in water studied by a hybrid supermolecule-polarizable continuum approach. **J. Am. Chem. Soc.** 122: 2621 -2627.

_____ , F. Zheng and D. W. Landry. 2003. Fundamental reaction mechanism for cocaine hydrolysis in human butyrylcholinesterase. **J. Am. Chem. Soc.** 125: 2462-2474.

Zhang, Y., J. Kua, and J. A. McCammon. 2002. Role of the catalytic triad and oxyanion hole in acetycholinesterase catalysis: ab initio QM/MM study. **J. Am. Chem. Soc.** 124: 10572-10577.

APPENDIX

The generation of charges of enzyme by the AMBER program

1. **To generate parameters for ligand**
   - partial optimization (optimized hydrogen atom) by using HF/3-21G or B3LYP/6-31G(d,p)
   - run single point calculation

     %Mem=100MW

     #p HF/6-31G(d) SCF=tight Test Pop=MK, iop(6/33=2) iop(6/42=6) sp

     ---RESP for ligand---

     0   1

     ....coordinate...........

   - get file.out with resp charges
   - calculation file.prepin

     antechamber –i file.out –fi gout file.prepin –fo prepi –at amber –c resp &
   - get file.prepin which consists of

     order, atom, atom-type, M/S/E, connecting atoms, B/A/Tvalues, charge

2. **To generate parameters for negative/positive charges**
   - partial optimization (optimized hydrogen atom) by using HF/3-21G or B3LYP/6-31G(d,p)
   - run single point calculation

     %Mem=100MW

     #p HF/6-31G(d) SCF=tight Test Pop=MK, iop(6/33=2) iop(6/42=6) sp

     ---RESP for ligand---

-/+(charge of ligand) 1

..........coordinate...........

- get file.out with resp charges
- extract esp charge from file.out (from GAUSSIAN)

  espgen –i file.out file.esp
- generate AC file

  antechamber –i file.out –fi gout –o file.ac –fo ac
- generate resp file from respgen

  respgen –i file.ac –o file.respin1 –f resp1

  respgen –i file.ac –o file.respin2 –f resp2
- check net charge (first line) and equivalent atom type
- run resp

  resp –O –I file.respin1 –o file.respout1 –e file.esp –t gout-stage1

  resp –O –I file.respin1 –o file.respout1 –e file.esp –q gout-stage1 –t gout-stage2

  get file charge 2 file but gout-stage2 file will be calculated in the next

step.
- Run antechamber

  antechamber –I file.ac –fi ac –o file.prepin –fo prepi –c rc –cf gout-stage2
- get file.prepin

3. **To generate parameter of the enzyme to get charges from AMBER**
   - generating file.frcmod

     parmchk –I file.prepin –f prepi –o file.frcmod

     We will get parameter to generate charges

   - loading enzyme and ligand
     - tleap

- source leaprc.ff99 (ff03 for AMBER8)

- #loadoff ../ca.off

- loadamberparmas file.frcmod

- loadamberprep file.prepin

- a=loadpdb file.pdb

- addIons a cl- 6

- addIons a Na+ 2

- solvatebox a WATBOX216 10.0

- save pdb a file.pdb

- save amberparm a file.top file.crd

- We will get charges from file.top to generate a set of point charges for electronic embeding method

This is an example of the charges of butyrylcholinesterase from file.top

10.0930	27.8940	55.9180	0.3881
8.8628	28.3092	57.5886	0.3116
8.9430	32.2580	57.0500	-11.0900
6.9066	29.2714	57.6808	-3.7192
4.5922	30.8221	58.0123	-16.7480
5.6090	32.4200	56.2080	0.3881
4.8410	32.9470	52.8340	2.6368
5.5348	34.6677	51.7154	2.3744
5.1190	30.2333	51.9741	1.6072
7.0950	34.2780	54.7570	-7.5750
6.0185	36.5710	55.9582	-4.2658
5.8890	36.7620	53.8460	7.7463
4.3595	37.8623	52.7988	-7.5750
10.1625	35.9066	55.6267	0.0784
12.8280	34.9210	56.3460	-0.0200
12.9220	34.2019	58.9867	5.8785
12.3665	31.6034	57.4756	-3.4732
12.8800	37.8400	59.7100	-3.4732
11.1090	38.5585	60.7140	3.0960
16.6890	38.4020	60.0960	13.3770
15.8216	37.6593	57.5123	1.7657
17.2600	39.4700	61.0400	1.4414
18.8839	40.7079	62.9523	-0.4592

20.1957	38.3762	63.3627	-7.5750
20.7600	38.9170	65.9100	-0.6250
20.4546	38.9733	67.9365	-3.1051
19.1204	41.0110	59.4397	-17.1420
18.8006	42.3043	57.1627	-0.4592
18.0951	43.8652	55.7295	-0.3153
14.9980	42.9280	58.7610	-0.4537
12.8510	42.1050	57.9530	-11.9280
10.4932	42.3942	58.6014	4.9546
7.9230	41.7110	57.5760	1.4414
8.6479	42.8252	59.2583	-7.5750
12.0330	40.8920	55.9180	-7.5094
11.9848	40.0297	53.4283	1.6801
14.6009	37.6095	52.3830	-10.3480
14.6072	40.2022	53.8886	-0.0656
9.3270	37.6170	51.7800	0.6414
7.3600	37.6640	50.0870	7.7463
6.2548	39.4761	49.8613	3.8577
4.2088	38.0324	46.3866	1.7821
10.0710	36.7430	50.7670	10.8840
10.6090	35.0242	48.8734	1.9097
9.7718	32.4471	48.1553	-10.8080
7.3916	33.4488	46.2046	-10.3480
7.3380	29.9870	43.8900	-10.3480
8.8950	30.0430	48.2700	0.3444
5.7200	28.2610	49.5360	-7.5750
6.4430	26.4050	50.9280	4.9546
6.6360	26.3070	46.9540	1.4414
7.0859	25.1014	43.8432	-7.5750
9.2027	24.0321	43.3926	-12.3200
10.8383	26.1756	44.7607	-14.9200
4.9916	23.4822	44.8820	-10.3480
3.7690	19.7270	45.9830	0.4610
2.2084	21.6005	45.4288	-7.5750
8.4920	19.2350	45.4930	0.6414
10.2569	19.9163	47.6090	-7.5750
11.8650	19.9878	45.0391	-10.3480
8.7821	16.9667	44.5996	-7.5750
10.1891	15.8326	47.7013	0.5376
10.6796	12.1655	50.4820	-7.5750
10.0930	12.5970	46.6480	10.8840
7.9102	16.2837	48.2999	0.4610
6.8530	16.3080	50.8730	-10.3480
5.6355	18.3583	51.5666	5.4394
6.4610	22.0210	49.9030	1.4414
3.6255	21.8025	49.9584	-10.8080
7.7200	22.6190	50.5430	-9.4082

9.7968	24.0858	51.2312	10.8840
12.9774	23.9575	49.0813	1.8350
11.3746	22.2188	50.9907	-10.3480
9.9590	27.9660	50.6370	-0.0911
8.7291	30.4489	51.0447	3.7574
11.3650	28.3760	50.2020	-4.3497
13.5246	29.3510	49.0754	-7.5750
12.7030	31.2700	48.7050	-7.5750
13.3415	33.7959	48.9609	1.0988
12.4530	34.1540	52.1390	-7.5750
10.6484	32.3694	54.4390	5.4394

This is an example of point charges of the butyrylcholinesterase framework for calculating in embedded method

N	35.7324	26.756	41.4085
H	34.7755	26.4128	41.3275
H	36.3201	26.0286	41.0001
N	39.5523	28.1211	39.7253
H	40.5674	28.1509	39.636
H	39.3317	27.1271	39.8011
N	39.168	25.2101	43.2812
H	38.4685	24.7703	43.8736
H	38.9776	24.962	42.3138
C	36.044	26.8642	42.832
H	37.1246	26.8934	42.9939
H	35.6475	27.8047	43.2402
C	35.4333	25.7471	43.6654
O	34.4808	25.0753	43.3317
O	36.0492	25.5929	44.8626
H	35.5507	24.9041	45.336
C	39.2027	28.7313	41.0081
H	39.4171	29.8074	40.9824
H	38.1282	28.6276	41.1844
C	39.9517	28.119	42.1887
O	39.3453	28.3539	43.3501
H	39.7553	27.7752	44.0441
O	40.9827	27.4839	42.0498
C	40.5169	24.8138	43.6645
H	41.1816	25.1582	42.861
C	40.7254	23.3039	43.877
H	40.0811	22.9282	44.6797

H	40.467	22.7739	42.9564
H	41.76	23.0657	44.1332
C	40.9705	25.6476	44.8635
O	42.0047	25.0934	45.5233
H	42.2556	25.7267	46.2179
O	40.5149	26.7236	45.2134
C	33.2885	23.8708	35.7889
O	33.9537	24.6312	36.8334
C	34.923	25.4446	36.4885
O	35.2683	25.6615	35.3209
C	35.4752	26.245	37.6669
C	35.0158	27.7142	37.4551
C	35.5705	28.7302	38.4753
C	36.9135	29.2342	37.866
C	37.0838	28.4357	36.5591
N	35.6445	28.1711	36.1338
C	34.9581	29.3204	35.4883
C	37.7478	27.0646	36.7537
C	37.0211	26.2513	37.8343
O	37.5733	24.9339	37.8619
C	38.0441	24.4774	39.0611
O	38.0689	25.1849	40.0641
C	38.5986	23.1111	38.9997
C	38.8998	22.47	40.2123
C	39.42	21.1815	40.2102
C	39.6478	20.5239	38.9972
C	39.355	21.1588	37.7907
C	38.8337	22.4506	37.7874
H	33.0539	24.5227	34.9456
H	33.9407	23.0514	35.4863
H	32.386	23.4858	36.2592
H	35.0357	25.8283	38.5746
H	33.9291	27.7561	37.3468
H	35.6892	28.2616	39.4592
H	34.8629	29.5549	38.5979
H	36.8705	30.3074	37.659
H	37.7777	29.0546	38.5139
H	37.5776	28.9968	35.7619
H	35.6128	27.3391	35.496
H	33.94	29.0232	35.2326
H	34.9345	30.1726	36.1667
H	35.4989	29.5881	34.5792
H	37.7628	26.5095	35.8103
H	38.7808	27.2301	37.0712
H	38.6946	22.982	41.1452
H	39.6308	20.6796	41.1497
H	40.0358	19.5098	38.9949

H	39.4963	20.6385	36.85
H	38.5766	22.9262	36.8514
H	37.2101	26.7087	38.8052
C	34.4514	23.1844	40.2376
O	35.4573	23.6809	39.369
H	34.1336	22.2198	39.9006
H	33.6174	23.8548	40.2377
H	35.4742	23.0802	38.5448
C	37.3845	16.0191	36.7175
C	36.1047	16.4852	37.4312
O	35.842	17.4946	37.0288
O	35.6781	15.8302	38.4094
H	37.3054	14.9771	36.4877
H	38.2278	16.1804	37.356
C	34.998	20.6325	35.4967
N	35.6207	20.0457	36.5781
C	34.9239	21.9767	35.7454
C	35.9368	21.0178	37.4469
N	35.525	22.2972	37.1217
H	35.7596	18.9605	36.7657
H	34.4749	22.7158	35.0968
H	36.4351	20.8567	38.3925
H	34.8446	23.104	41.2294
H	37.5109	16.5754	35.8123
H	34.6385	20.1296	34.6233

26.6970	36.1150	36.8790	0.1088
31.6900	36.8720	36.2100	0.0039
33.0300	38.2220	38.2580	-0.0568
29.6300	35.8060	35.0350	0.0496
30.8370	35.3700	31.9690	-0.1035
34.2530	32.9160	28.5590	-0.1675
29.6570	32.2100	28.3100	-0.0758
24.5680	22.8760	30.5000	-0.0299
25.9700	19.6570	31.5270	-0.0474
24.8370	19.1200	34.7180	0.0264
23.7360	26.6280	32.1900	-0.1035
27.0310	31.3250	31.8290	0.0039
25.0390	24.1580	44.1610	-0.0474
26.7370	28.2390	48.1050	-0.1035
30.3570	28.1760	47.4280	0.0237
29.4670	30.1310	47.2270	0.0161
29.7170	26.8570	49.9100	0.0034
27.2440	30.1220	43.5400	-0.0427
25.9590	28.4810	44.8110	-0.0427
25.3280	31.4400	41.1790	-0.1232
24.8080	29.1760	42.3100	0.0496
24.1760	28.8070	35.2170	-0.0751

24.1500	24.6400	40.1460	-0.0002
24.5060	25.3480	38.9830	-0.0347
29.9290	32.4660	45.9950	0.0310
32.3980	37.3080	42.5320	-0.0481
33.2630	36.1400	42.0420	0.1338
37.1130	37.3880	37.7490	-0.0758
35.2540	38.9540	36.4570	0.0110
36.1020	39.2470	40.6850	0.0496
40.3510	37.1740	41.5900	-0.0063
41.2510	36.3710	44.0500	0.0242
35.7640	36.0360	46.8830	0.1088
35.8720	34.4330	48.9790	0.0168
39.5270	32.7780	50.0060	-0.0751
32.6490	33.1270	48.9790	-0.0118
34.4130	32.2740	47.5110	-0.1714
35.0550	23.6260	51.7690	-0.0582
33.6350	25.9420	49.6870	0.0144
38.3040	24.7350	50.5150	-0.0758
41.4030	23.4340	50.0820	0.0064
40.8620	29.1370	50.6620	-0.0201
41.4300	30.0100	48.3670	-0.0751
43.4800	28.2270	50.4520	0.0182
34.9490	29.7370	51.8060	0.0375
32.9230	19.2320	50.1690	0.1088
35.4580	20.8540	50.3270	-0.0066
37.6000	21.0460	50.1450	-0.0751
35.2080	17.3900	46.9690	-0.1035
31.9500	17.7470	46.9750	0.0064
30.3790	19.8650	46.5370	0.0775
44.9370	25.6370	49.3000	-0.0229
46.7600	24.7210	45.4850	0.0191
44.9570	21.1830	46.3020	-0.1081
47.4270	23.0670	43.4820	-0.1035
50.0430	23.5220	39.3970	0.0046
48.0390	30.7380	44.9030	-0.0582
46.7270	32.4770	41.8040	-0.0758
46.1430	35.2240	41.3470	0.0008
45.3410	34.0330	39.8600	-0.1232
33.7620	38.4170	33.4560	-0.0751
39.5130	38.7140	33.2450	0.0025
38.0950	36.8340	33.7130	-0.1492
46.4280	32.4000	31.0970	0.0039
46.5810	25.8840	26.8560	0.0184
48.1530	26.6070	30.0860	0.0117
43.7100	27.2240	26.9390	-0.1035
44.1190	22.6730	27.1040	0.0034
41.9570	22.5970	27.0040	0.0046

42.7640	30.7350	28.5350	0.0064
43.1780	37.1690	33.6720	-0.0372
42.3660	37.0390	31.3830	-0.1675
40.8230	37.2680	38.0860	0.0054
45.1420	33.1750	44.0160	-0.1047
48.3970	26.4740	46.2780	0.0039
39.3810	16.2650	48.0600	0.0144
36.0360	15.2990	46.2120	0.0496
34.7810	12.7330	40.5960	0.1088
32.9990	11.7960	38.7050	0.0191
31.0550	13.8600	37.8550	-0.1081
36.0640	11.5610	37.8650	-0.1035
36.8400	12.2640	34.0680	0.0069
37.6710	12.9560	31.7490	0.1457
39.1690	17.0940	28.2440	0.0184
37.5750	18.4980	27.0450	-0.1035
28.9450	20.4190	27.6820	0.0287
32.7150	20.7470	26.7460	-0.0435
39.3530	21.0120	26.7100	-0.0758
41.2160	19.1820	26.3730	0.0083
37.5190	19.8450	25.2410	0.0496
36.5110	18.0760	24.6430	0.0144
36.0330	22.7750	24.3070	-0.0758
33.8660	23.6940	25.6130	0.0110
37.4870	25.5250	24.8440	-0.0758
39.7900	26.4350	24.9120	0.1088
42.3850	25.7410	24.1600	0.0150
46.7920	16.1560	32.3060	-0.1035
44.2240	18.4380	29.6440	0.0544
44.3300	17.7250	32.1050	0.1088
44.9760	14.9040	33.6320	0.0535
46.4790	16.3030	37.4640	-0.1060
48.6800	18.7660	34.6880	-0.0028
43.4660	13.6290	38.6470	0.0237
41.5890	11.7520	37.5560	0.0034
46.1500	14.9960	40.1160	-0.0758
44.3260	17.2110	43.6420	-0.0758
42.3160	15.4950	43.0640	0.0110
44.5910	14.5620	44.7470	-0.0758
44.0090	17.8790	47.5910	0.0054
41.9470	18.4430	48.9680	-0.0229
32.3980	14.9940	44.0900	-0.1017
28.9330	16.0160	29.6950	-0.0474
27.3220	18.7300	28.3490	0.0264
30.1370	12.4480	34.1210	0.0144
31.5010	14.6730	32.5250	0.0496
31.9820	16.9290	27.7160	-0.0098

29.4730	15.6940	34.2950	0.0054
26.6980	16.0740	37.2840	-0.1035
28.8030	13.9680	40.4710	0.0102
29.8430	14.3270	42.2840	-0.0077
25.9680	19.1320	40.1520	0.0237
24.3040	20.9420	38.7870	0.0034
24.7660	20.4420	44.4150	-0.0311
27.3110	36.5260	35.8950	-0.1035
28.7430	36.8390	39.9210	-0.0224
29.7410	36.2760	37.6770	0.1088
31.9250	37.6920	35.5310	0.0205
34.0530	37.7660	38.9750	0.0352
34.6630	33.1120	27.6570	0.0765
30.3310	32.7490	27.7860	0.0496
23.0640	23.7450	32.3780	-0.0009
24.3780	23.7910	29.9390	0.0376
26.5790	19.2660	30.7120	0.0287
24.3580	20.8320	33.5130	-0.0435
25.6930	29.7910	31.0770	0.0035
26.1250	30.4630	33.0950	0.0039
24.3230	24.1530	43.3400	0.0287
26.7150	24.2210	46.4120	-0.0435
28.3460	26.6930	47.7480	-0.0758
31.2010	27.3290	48.4120	-0.0078
31.3990	26.6520	50.4550	0.0034
27.4690	31.1610	43.2980	0.0302
25.2060	28.2460	45.5640	0.0302
25.1120	31.5010	38.8170	-0.0444
25.3330	32.3990	41.1420	0.0748
22.6910	27.3760	37.0370	0.0083
23.9010	28.2420	34.3260	0.0182
25.0610	23.7150	40.6970	-0.0347
23.7800	26.0090	38.5090	0.0310
26.9250	33.6340	44.4010	0.0191
25.7130	34.0280	41.9620	-0.1081
31.1670	34.9250	46.0480	-0.0028
33.4950	34.5210	44.6700	0.0310
30.6800	36.1300	43.8610	0.1088
31.6710	37.4500	41.7320	0.0284
36.4700	40.0050	35.6930	0.0110
35.1890	40.1490	37.9700	0.0496
38.8990	39.1340	41.8490	-0.0758
39.9030	36.9490	40.6220	0.0054
39.5770	35.2150	44.8020	-0.0311
34.9630	35.1100	46.7540	-0.1035
38.0130	34.5430	49.1510	-0.0201
37.1530	32.1920	49.7340	-0.0751

31.5980	32.9050	48.7950	0.0064
29.8150	22.9980	49.2850	0.1088
36.1040	25.8030	50.8700	-0.0160
32.9600	24.4420	50.3650	0.0144
39.9890	22.3580	50.1730	0.0064
40.2760	26.7420	51.0010	-0.0758
39.8270	29.3010	50.3640	0.0083
41.6420	30.9930	48.7880	0.0182
43.8030	28.8570	48.8200	0.0182
38.3400	27.9230	52.3770	0.0496
34.9700	30.2340	50.8360	0.0254
32.4710	20.3370	49.8590	-0.1035
36.1450	19.4240	48.8760	-0.0201
36.4570	19.2780	51.4080	-0.0751
37.5370	21.7530	49.3180	0.0182
29.8660	17.9120	46.5250	0.1267
44.9940	26.7130	49.1350	0.0242
44.8100	22.8630	49.6990	-0.0311
46.7880	22.7360	46.3150	-0.0372
46.9250	20.3740	45.7590	-0.1675
46.4340	30.3370	42.9660	-0.0160
47.3060	31.3790	45.3920	0.0144
47.0920	28.3920	45.7690	0.0144
45.7780	32.6540	42.1010	0.0496
47.1530	35.4580	39.4600	-0.0444
44.7640	34.7350	39.5500	0.0748
48.6280	32.6830	36.1400	0.0816
33.6300	38.7510	34.4850	0.0182
31.1730	38.0790	32.8750	0.0182
40.5160	38.8650	32.8460	-0.0077
38.4270	36.2730	28.2240	0.0150
44.1450	33.1340	27.5400	0.0144
45.6850	34.3070	30.3760	0.0035

CURRICULUM VITAE

NAME	**:**	Mr. Narongsak Arayalert
BIRTH DATE	**:**	Novenber 7, 1979
BIRTH PLACE	**:**	Pratumthani, Thailand
EDUCATION	**:**	**YEAR** **INSTITUTION** **DEGREE/DIPLOMA**
		2001 Kasetsart University B.S. (Chemistry)

SCHOLARSHIP/AWARDS

: Scholarship from The Development and Promotion of Science and Technology talented project (DPST) (2001-2004)

: Scholarships from the Postgraduate on Education and research in Petroleum and Petrochemical Technology (ADB-MUA) (2002-2003)